AD-A177 305 EXAMINATION OF MECHANISMS AND FUEL-MOLECULAR EFFECTS ON SOOT FORMATION..(U) UNITED TECHNOLOGIES RESEARCH CENTER EAST HARTFORD CT M B COLKET ET AL. 10 DEC 86 1/1

UNCLASSIFIED UTRC/R86-957047 AFOSR-TR-87-0117 F/G 21/2 NL

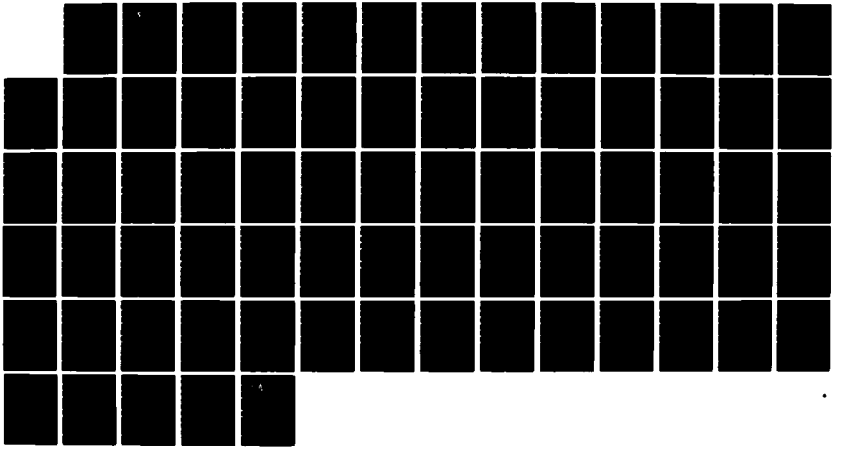

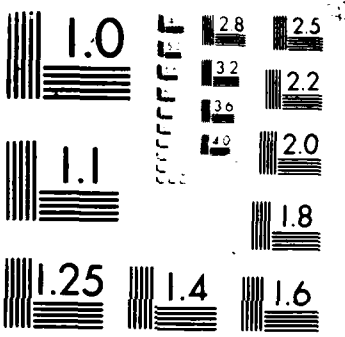
1.0
1.1
1.25
1.4
1.6
2.8
3.2
3.6
4.0
2.5
2.2
2.0
1.8

Unclassified
SECURITY CLASSIFICATION OF THIS PAGE

1a. REPORT SECURITY CLASSIFICATION: Unclassified	
2a. SECURITY CLASSIFICATION AUTHORITY	3. DISTRIBUTION/AVAILABILITY OF REPORT: Distribution unlimited; approved for public release
2b. DECLASSIFICATION/DOWNGRADING SCHEDULE	
4. PERFORMING ORGANIZATION REPORT NUMBER(S)	5. MONITORING ORGANIZATION REPORT NUMBER(S): AFOSR-TR- 87-0117
6a. NAME OF PERFORMING ORGANIZATION: UNITED TECHNOLOGIES RESEARCH CENTER	6b. OFFICE SYMBOL (If applicable):
7a. NAME OF MONITORING ORGANIZATION: Air Force Office of Scientific Research	
6c. ADDRESS (City, State and ZIP Code): EAST HARTFORD, CONNECTICUT 06108	7b. ADDRESS (City, State and ZIP Code): Bolling AFB DC 20332-6448
8a. NAME OF FUNDING/SPONSORING ORGANIZATION: Air Force Office of Sci. Res.	8b. OFFICE SYMBOL (If applicable): AFOSR/NA
9. PROCUREMENT INSTRUMENT IDENTIFICATION NUMBER: F49620-85-C-0012	
8c. ADDRESS (City, State and ZIP Code): Bolling AFB DC 20332-6448	10. SOURCE OF FUNDING NOS

PROGRAM ELEMENT NO.	PROJECT NO.	TASK NO	WORK UNIT NO
61102F	2308	A2	

11. TITLE (Include Security Classification): (UNCLASSIFIED) EXAM. OF MECH. OF FUEL EFFECTS ON SOOT FORM.

12. PERSONAL AUTHOR(S): M. B. Colket, III, D. J. Seery, J. J. Sangiovanni

13a. TYPE OF REPORT	13b. TIME COVERED	14. DATE OF REPORT (Yr., Mo., Day)	15. PAGE COUNT
Annual	FROM 11/25/85 TO 11/24/86	December 10, 1986	72

16. SUPPLEMENTARY NOTATION

17. COSATI CODES			18. SUBJECT TERMS (Continue on reverse if necessary and identify by block number)
FIELD	GROUP	SUB GR	Hydrocarbon pyrolysis, acetylene, vinylacetylene, ethene styrene, 1,3,5-hexatriene, biacetyl, soot formation

19. ABSTRACT (Continue on reverse if necessary and identify by block number)

A variety of hydrocarbons has been pyrolyzed in a single-pulse shock tube over the temperature range of 1001 to 2400 K and for dwell times of 500 to 700 microseconds. Gas samples of reactant, intermediate, and final products were collected and analyzed using gas chromatography. Experimental data were used in conjunction with a computer model to develop or confirm existing detailed chemical kinetic models for several of the hydrocarbons that were pyrolyzed. Model results agreed well with experimental data not only for the decomposition of the parent compound and formation of low molecular weight products, but also for the formation of single-ring aromatic species. These latter processes are believed to lead to the formation of polycyclic aromatic hydrocarbons, soot precursors, and eventually soot. Specific mechanisms and rate coefficients for the formation of aromatic rings have been proposed.

20. DISTRIBUTION/AVAILABILITY OF ABSTRACT	21. ABSTRACT SECURITY CLASSIFICATION
UNCLASSIFIED UNLIMITED ☒ SAME AS RPT ☐ DTIC USERS ☐	Unclassified

22a. NAME OF RESPONSIBLE INDIVIDUAL	22b. TELEPHONE NUMBER (Include Area Code)	22c. OFFICE SYMBOL
Julian M. Tishkoff	(202)767-4935	AFOSR/NA

DD FORM 1473, 83 APR EDITION OF 1 JAN 73 IS OBSOLETE.

Unclassified
SECURITY CLASSIFICATION OF THIS PAGE

R86-957047

Examination of Mechanisms and Fuel-Molecular Effects on Soot Formation

TABLE OF CONTENTS

R86-957047

Examination of Mechanisms and Fuel-Molecular Effects on Soot Formation

LIST OF TABLES

R86-957047

Examination of Mechanisms and Fuel-Molecular Effects on Soot Formation

Annual Report

I. SUMMARY

A variety of hydrocarbons has been pyrolyzed in a single-pulse shock tube over the temperature range of 1000 to 2400 K and for dwell times of 500 to 700 microseconds. Gas samples of reactant, intermediate, and final products were collected and analyzed using gas chromatography. Experimental data were used in conjunction with a computer model to develop (or confirm existing) detailed chemical kinetic models for several of the hydrocarbons that were pyrolyzed. Model results agreed well with experimental data not only for the decomposition of the parent compound and formation of low molecular weight products, but also for the formation of single-ring aromatic species. These latter processes are believed to lead to the formation of polycyclic aromatic hydrocarbons, soot precursors, and eventually soot. Specific mechanisms and rate coefficients for the formation of aromatic rings have been proposed.

II. INTRODUCTION

The production of soot in diffusion flames, such as that existing in gas turbine engines, is directly related to the chemical nature of the fuel. In addition, research has shown recently that chemical kinetic processes control the growth of polynuclear aromatics and probably the formation of soot precursors. The production rate of soot precursors, in turn, limits the production rate of the number of soot particles and hence effects the total mass of soot produced. This work focuses on obtaining experimental data on the pyrolysis and oxidative pyrolysis of hydrocarbons under soot-forming conditions. A single-pulse shock tube has been selected for the experimental tool since it is one of the few devices capable of obtaining detailed information on product distribution over the range of 1200 to 2400 K in an environment free from complications due to diffusional effects. Using the experimental data and single-pulse information obtained from other work, detailed chemical kinetic mechanisms describing the pyrolysis of a variety of hydrocarbons are being developed. Chemical mechanisms describing the formation of aromatic hydrocarbons (from aliphatic hydrocarbons) are included in the model.

III. STATEMENT OF WORK

United Technologies Research Center (UTRC) shall furnish the level of effort including all related services, facilities, supplies and materials, needed to:

a. Select a variety of hydrocarbon fuels for pyrolysis and oxidative pyrolysis. The selection will be subject to approval by the AFOSR technical manager and will be based in part on preliminary results from the experimental and modeling phases of this program.

b. Pyrolyze and/or oxidatively pyrolyze a variety of hydrocarbons and/or mixture of hydrocarbons in the single-pulse shock tube. Test conditions will vary from approximately 1200 to 2500 K, dwell times of 500 to 800 microseconds, and total pressures of 4 to 8 atmospheres. Approximately 18-22 mixtures will be shock-heated and examined. For each mixture, approximately twenty individual shocks will be run.

c. Examine data and quantitatively determine concentrations of parent hydrocarbons, intermediates and final products; collate the data from each series of runs and prepare data for analysis; estimate soot and/or PAH formation based on mass balance of observable species.

d. Evaluate experimental data to determine chemical mechanisms and kinetic rates.

e. Identify species and mechanisms leading to the formation of soot (or soot precursors).

f. Develop detailed chemical kinetic mechanisms and operate a shock tube version of the CHEMKIN code.

g. Construct a detailed model describing soot formation and growth in a diffusion-free environment.

h. Make comparisons between experimental data and model predictions.

i. Incorporate recent advances in the chemical kinetics of hydrocarbon pyrolysis and pre-particle mechanisms of soot formation into computer models.

IV. STATUS OF WORK

(A) Experimental Effort

Seventeen separate series of single-pulse shock tube experiments were completed during the first year of this contract using both contract (AFOSR) and Corporate (UTRC) funds (see Table I). During this past, second year, ten new series of experiments were completed under contract sponsorship and eight under Corporate sponsorship. Initial reactant concentrations for these eighteen experiments are listed in Table II. Each series represents a collection of individual shock tube experiments along with chemical analysis of reactant and products for a given initial reactant condition (species, initial concentration). Shock strengths were varied to produce a range in initial post-shock temperature from approximately 1100 to 2400 K.

Experiments performed during this past year include the pyrolysis and fuel-rich oxidation of ethene. Experimental data are reproduced in Figs. 1a-3a for the pyrolysis and Figs. 4-8 for the fuel-rich oxidation of about 3 1/2 percent ethene in argon. Preliminary modeling results for the pyrolysis are included in Figs. 1b-3b, using a chemical kinetics sequence slightly modified from that presented in Appendix I. Of particular interest to soot formation is the fact that with oxygen addition, peak concentration levels for each of the single ringed aromatic species are nearly the same as observed during pyrolysis; however these peak concentrations occur at 1300 to 1400 K which is approximately five hundred degrees below the temperature at which the peaks occur with pyrolysis. Other interesting features during oxidation include high formation rates of methane and a high CO/C_2H_2 ratio. The presence of methane indicates the importance of methyl radicals during oxidation whereas the high CO/C_2H_2 ratio substantiates suggestions that ethene and/or vinyl radicals decompose via addition of oxidative radicals (O or OH) rather than extraction of H-atom by such radicals. Detailed modeling of these results will continue into next year.

Other experiments completed last year include pyrolysis of styrene (an alkylated aromatic) and 1,3,5-hexatriene. Styrene was selected due to its poential role in the growth from single to double ring aromatics. The linear six-membered aliphatic, 1,3,5-hexatriene, was selected since it is the parent of two radical intermediates, i.e., 1,3,5-hexatrien-1-yl and 1,3,5-hexatrien-3-yl which have been postulated as intermediates in the production of benzene from alipatics. Data from 1,3,5-hexatriene have not yet been reduced. The data from the styrene experiments have been reduced although there is some difficulty in interpretation due to a $\pm$ 15 percent uncertainty in the ability to accurately measure styrene. Below 1400 K, there is relatively little decomposition of the aromatic ring although styrene does decompose principally to benzene, phenylacetylene, hydrogen, ethene and acetylene. At these temperatures, there is a slight preference to form phenylacetylene but the trend is opposite at higher temperatures. At 1450 K and above, there is rapid loss of the initial styrene although there is not a compensorate production of low molecular weight products. Presumably the styrene is converted to unobservable high molecular weight species. Mechanisms describing this phenomena are under investigation and they may be related to the formation of soot precursors.

TABLE I

SERIES OF EXPERIMENTS COMPLETED
DURING FIRST YEAR OF PROGRAM

Reactant	Initial Concentration (%)
Benzene, C_6H_6	0.12
Benzene, C_6H_6	0.012
Vinylacetylene, C_4H_4	1.0
Vinylacetylene, C_4H_4	0.11
Vinylacetylene C_4H_4	0.01
C_2H_2/C_6H_6	0.82/0.06
C_2H_2/C_6H_6	0.115/0.0085
C_2H_2/C_6H_6	0.016/0.0012
Acetylene	4.9
Acetylene	0.6
Acetylene	0.069
Toluene, C_7H_8	* 0.05
Toluene, C_7H_8	* 0.035
Toluene, C_7H_8	* 0.016
Toluene, C_7H_8	* 0.0175
C_2H_2/C_7H_8	* 3.3/0.51
Acetaldehyde, CH_3CHO	* 0.105

All fuels were diluted in argon and (except for the experiments on pure toluene) were conducted at total pressures of approximately six to nine atmospheres.

* Research conducted under Corporate-sponsored program.

TABLE II

SERIES OF EXPERIMENTS COMPLETED
DURING SECOND YEAR OF PROGRAM

Reactant	Initial Concentration %
Ethene, C_2H_4	3.5
Ethene, C_2H_4	0.3
Ethene, C_2H_4	0.05
Styrene, C_8H_8	0.4
Styrene, C_8H_8	0.2
C_2H_4/O_2	3.3/2.05
C_2H_4/O_2	0.22/0.13
1,3,5-Hexatriene, C_6H_8	1.0
1,3,5-Hexatriene, C_6H_8	0.09
Acetaldehyde, CH_3CHO	* 0.01
Biacetyl, $(CH_3CO)_2$	* 0.22
Biacetyl, $(CH_3CO)_2$	* 0.022
$C_2H_2/(CH_3CO)_2$	* 3.5/0.18
$C_2H_2/(CH_3CO)_2$	* 0.3/0.15
Toluene, C_7H_8	* 1.0
Toluene, C_7H_8	* 0.1
Toluene, C_7H_8	* 0.01

* Research conducted under Corporate-sponsored program

Related to the experimental work is a computer code which has been written recently to help organize, document, and plot experimental data.

(B) Model Effort

(1) Code Enhancement

Much of the enhancement to the computer codes for development of models used in this contract have been made under a Corporate-sponsored program. Yet the advancements will enhance significantly the rate of progress in the present contract work and therefore will be described briefly.

Chemical kinetic modeling is performed using CHEMKIN, LSODE, and a shock tube code for CHEMKIN originally written by personnel at Sandia National Laboratories. As described in the proposal for this contract, the original shock tube code had already been modified in-house in order to model the quenching process in a single-pulse shock tube. As described in the first annual report for this contract, additional modifications have been made to plot species concentrations and reaction contributions to the formation/destruction of each species. During the past year, the code has been modified or a new code developed to:

1. Identify the principal initiation and termination reactions and their respective rates.

2. Identify reactions which are (nearly) equilibrated.

3. Identify whether certain reactions proceed principally in the forward or reverse directions.

These new capabilities may not appear as highlights in a publication or a presentation, but are of great value to meeting the overall research objectives of this contract.

(2) Chemical Kinetic Modeling

Detailed chemical kinetic modeling has been performed for ethene pyrolysis and previous modeling for acetylene, vinylacetylene and benzene was revised. In addition, modeling for biacetyl (see Appendix II) and acetaldehyde has been performed under Corporate sponsorship. The chemical kinetic modeling for the pyrolysis of acetylene and vinylacetylene is described in detail in Appendix I; of particular interest to the present work are the low and high temperature sequence of steps describing formation of an aromatic ring for alphatic species. The specific reaction sequences and rate coefficients used in the model are summarized in Table III.

The modeling results for ethene pyrolysis (Figs 1b-3b) were obtained using the chemical kinetic sequence listed in Appendix I with a few additional reactions to account for the dominance of ethene. The model as yet does not include mechanisms for the formation of methane (CH_4), or the C_3- and C_5-hydrocarbons; in addition, ethane formation mechanisms are limited.

TABLE III

REACTIONS AND RATE COEFFICENTS FOR STEPS
LEADING TO FORMATION OF AROMATIC RING

Low Temperature Sequence

	Log A	E/1000
$H + C_2H_2 \rightleftarrows C_2H_3$	12.74	2.5
$C_2H_3 + C_2H_2 \rightleftarrows n\text{-}C_4H_5$	12.05	4.0
$n\text{-}C_4H_5 + C_2H_2 \rightleftarrows$ [illegible]$\text{-}C_6H_7$	12.81	9.0
[illegible]$\text{-}C_6H_7 \rightleftarrows c\text{-}C_6H_7$	11.36	0.4
$c\text{-}C_6H_7 \rightleftarrows C_6H_6 + H$	13.12	24.6

High Temperature Sequence

$H + C_2H_2 \rightleftarrows C_2H + H_2$	13.6	20.5
$C_2H + C_2H_2 \rightleftarrows n\text{-}C_4H_3$	13.56	3.0
$n\text{-}C_4H_3 + C_2H_2 \rightleftarrows$ [illegible]$\text{-}C_6H_5$	11.71	-0.1
[illegible]$\text{-}C_6H_5 \rightleftarrows c\text{-}C_6H_5$	10.22	1.4
$c\text{-}C_6H_5 + H_2 \rightleftarrows C_6H_6 + H$	12.39	9.5
$c\text{-}C_6H_5 + C_2H_2 \rightleftarrows C_8H_6 + H$	12.00	4.0

$k = A \exp(-E/RT)$

Units: A, cc, mole, sec

E, cal/mole/K

Consequently model predictions are not available for these species. For the other species, however, the agreement between the model and experiments are quite satisfactory considering that the mechanism from Appendix I (developed for pyrolysis of acetylene and vinylcetylene) was used intact with only a few added reactions whose rate constants were obtained from the literature. No 'fitting' of rate constants was performed. Additional work remains to include species not presently accounted for by the model.

V. LIST OF PUBLICATIONS

A paper entitled "The Pyrolysis of Acelylene and Vinylacetylene in a Single-Pulse Shock Tube" by M. B. Colket has been accepted for publication in the Twenty-First Symposium (International) on Combustion (see Appendix I).

An article entitled "Single-Pulse Shock Tube Examination of Hydrocarbon Pyrolysis and Soot Formation" by M. B. Colket has been published in Shock Waves and Shock Tubes, Proceedings of the Fifteenth International Symposium on Shock Wave and Shock Tubes, Edited by D. Bershader and R. Hanson, p. 311, Stanford University Press, Stanford, California 1986 (see Appendix I of First Annual Report, UTRC R85-957047).

A manuscript entitled "Pyrolysis of Biacetyl in a Single-Pulse Shock Tube" has been completed under Corporate sponsorship and will be submitted to the Journal of Physical Chemistry (see Appendix II).

VI. MEETING INTERACTIONS

In addition to the meetings listed in the first annual report (UTRC R85-957047) the Principal Investigator of this program attended the following meetings during this past year.

1. Twenty-first Symposium (International) on Combustion in Munich, W. Germany, August 1986. A paper entitled "The Pyrolysis of Acetylene and Vinylacetylene in a Single-Pulse Shock Tube" was presented by M. B. Colket. In addition M. Colket served as Poster Chairman and member of the Program Advisory Committee, the Program Sub-committee and the Publications Committee.

2. The 1986 Spring Technical Meeting of the Central States Section of the Combustion Institute in Cleveland, Ohio, May 1986. A paper entitled "Formation of C_2-hydrocarbons and Benzene from Pyrolysis of Biacetyl" was presented by M. B. Colket.

3. Department of Energy, Basic Sciences Contractors Meeting, Arlie House, Va, May 1986. M. Colket was invited by Dr. A. Laufer to be an observer and participant in discussions at the D.O.E. meeting.

VII. NEAR-TERM PLANS

Two experimental modifications, one minor and one major, are being considered. Much of these modifications are expected to be completed under Corporate sponsorship; but both changes are expected to significantly add to the experimental capability of the present research and any future program. The minor change is a procedure by which a filter/trap will be placed at the location where gas samples are extracted from the shock tube. After gas collection, the trap will be removed and flash heated in a carrier line leading to a gas chromatographic column. In this manner, it is hoped that higher molecular weight species can be detected and identified. The major modification is to couple a time-of-flight mass spectrometer (TOF/MS) to the end of the shock tube, while simultaneously collecting gas samples for gas chromatographic analysis. Data from the TOF/MS will be collected using high speed A/D convertors. Using this arrangement, it is expected that real-time data, including measurement of radical intermediates can be obtained. With this information confidence in the modeling should be increased substantially. The analysis by TOF/MS will probably not be completed fully in time to enhance significantly the present program but should be available for further research in the area of soot kinetics and/or hydrocarbon combustion.

Additional experiments are planned for hydrocarbon oxidation and for the pyrolysis of high-purity allene. (Previous results are clouded by the use of commercially available allene which is typically only 90% pure.)

Chemical kinetic modeling will be continued with particular emphasis on PAH growth during oxidation of hydrocarbons. In addition to the chemical kinetic model, a computer model describing the condensation, growth, and agglomeration of soot in a diffusion-free environment will be developed durng the next year.

3.5% ETHENE PYROLYSIS, ALIPHATICS

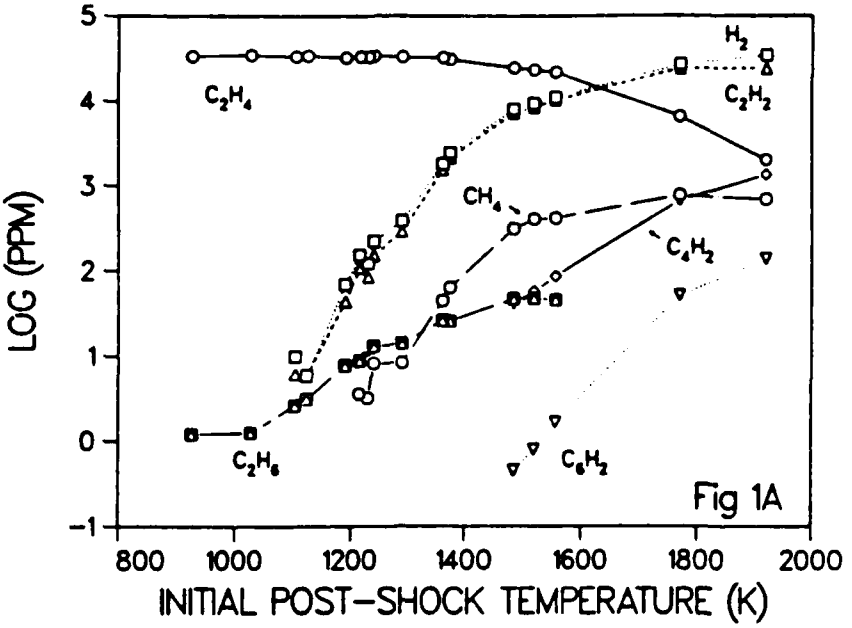

3.5% ETHENE PYROLYSIS, MODEL

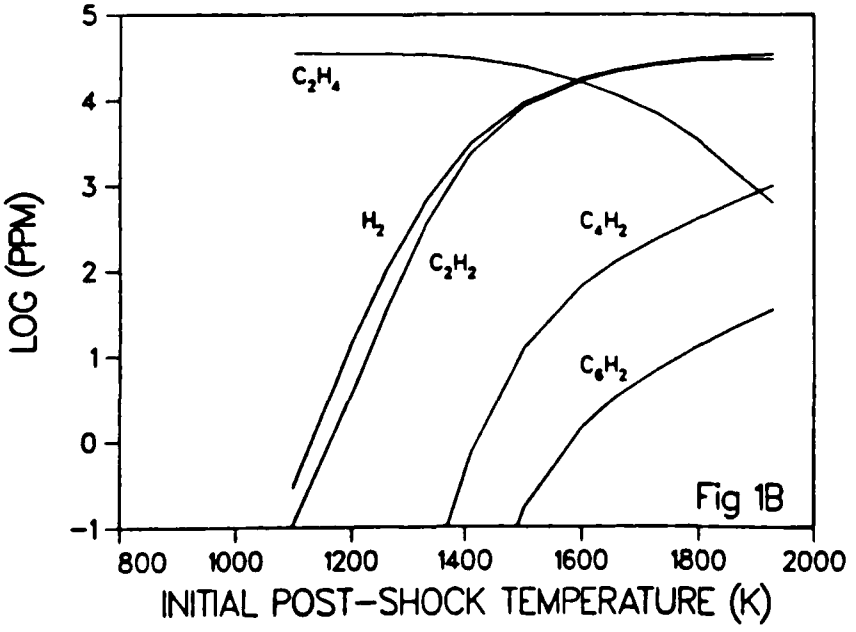

3.5% ETHENE PYROLYSIS, ALIPHATICS

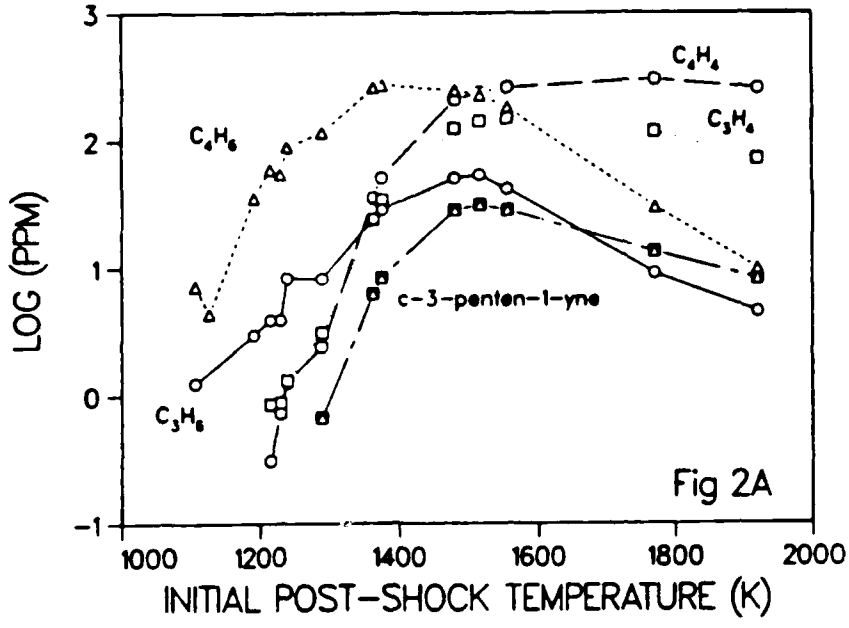

3.5% ETHENE PYROLYSIS, MODEL

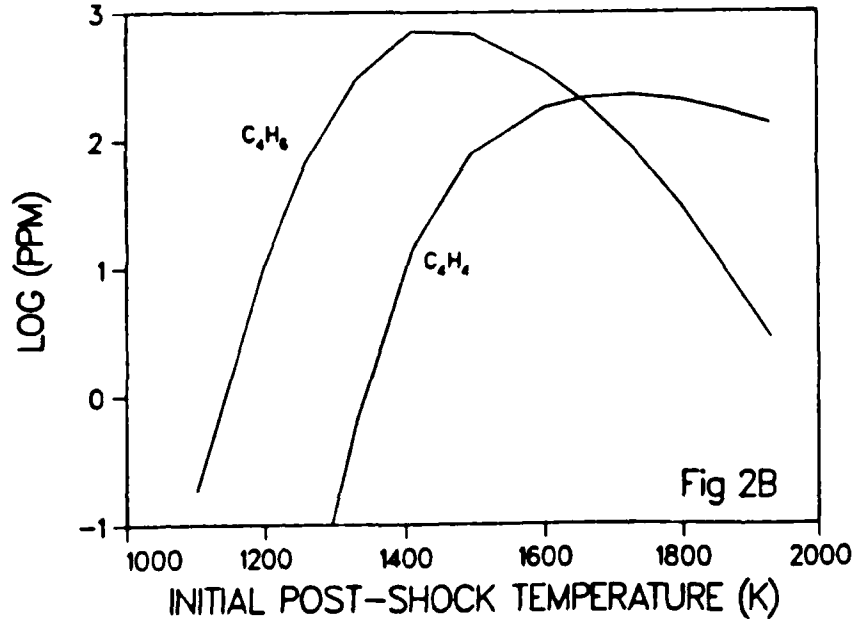

3.5% ETHENE PYROLYSIS, AROMATICS

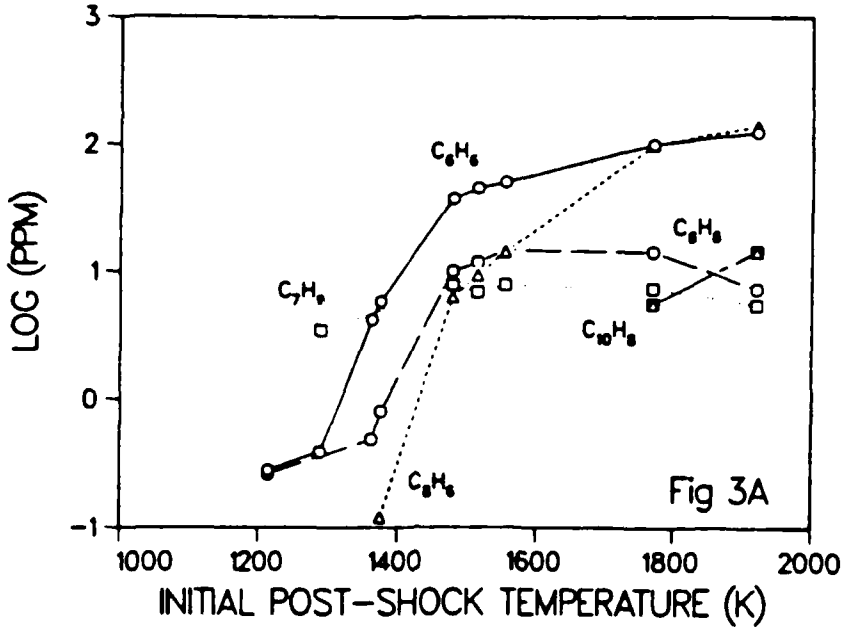

3.5% ETHENE PYROLYSIS, MODEL

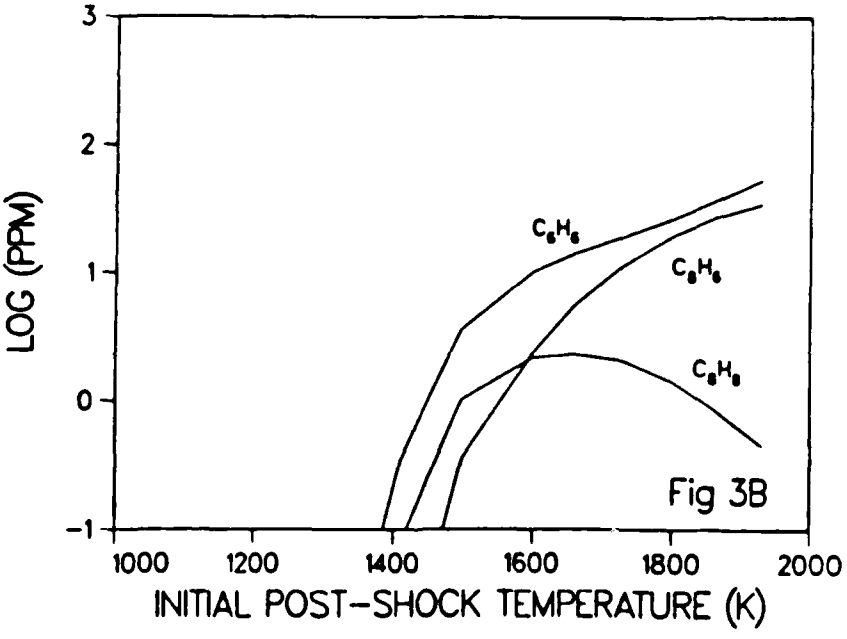

3.3% ETHENE, 2.05% OXYGEN

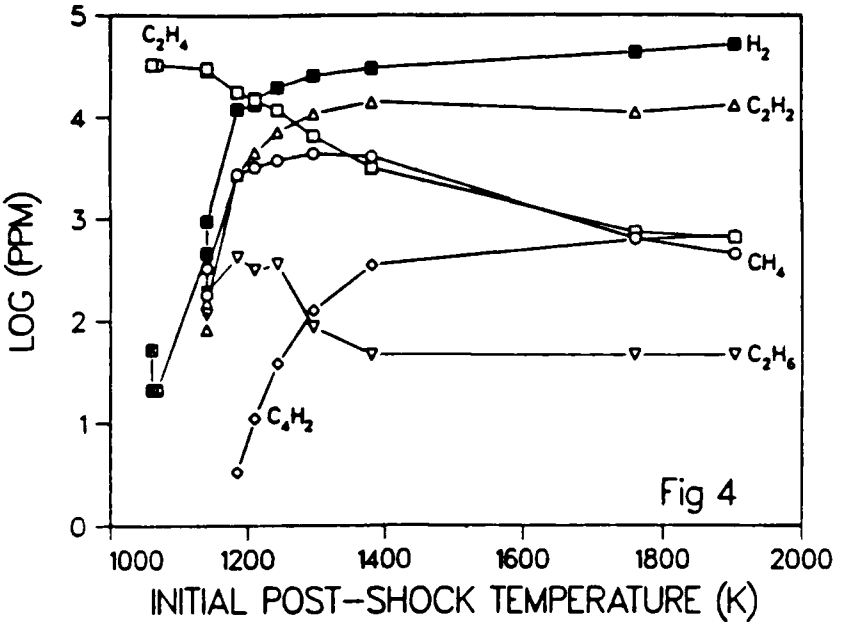

3.3% ETHENE, 2.05% OXYGEN

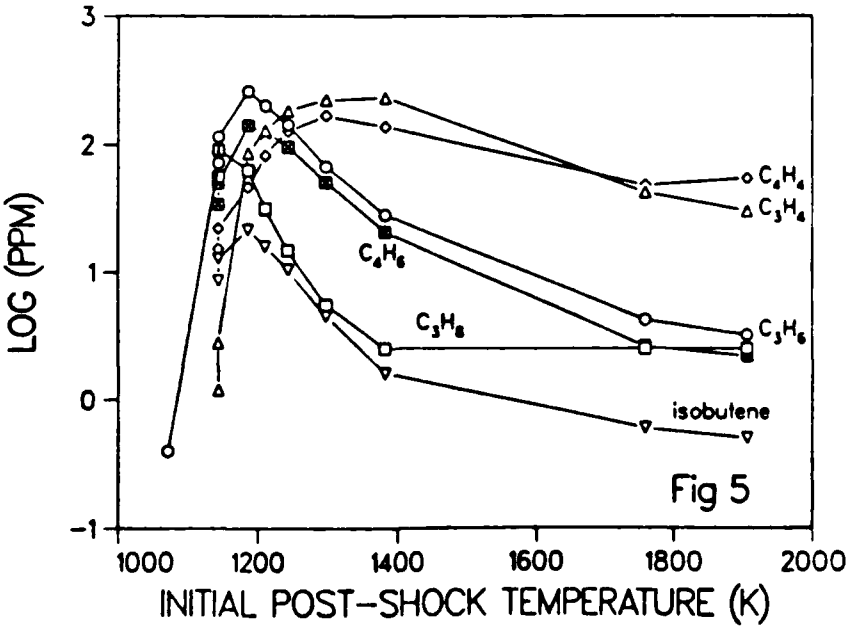

3.3% ETHENE, 2.05% OXYGEN

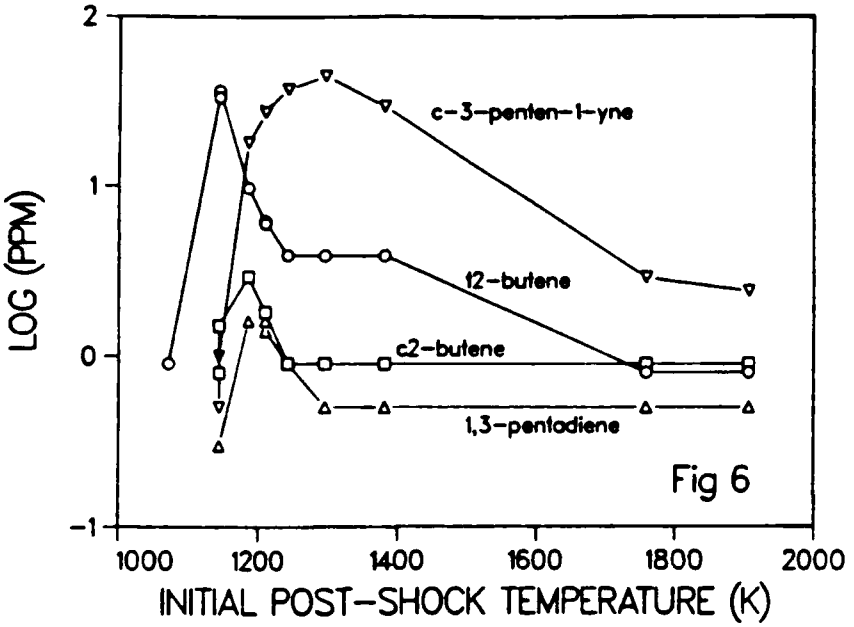

3.3% ETHENE, 2.05% OXYGEN

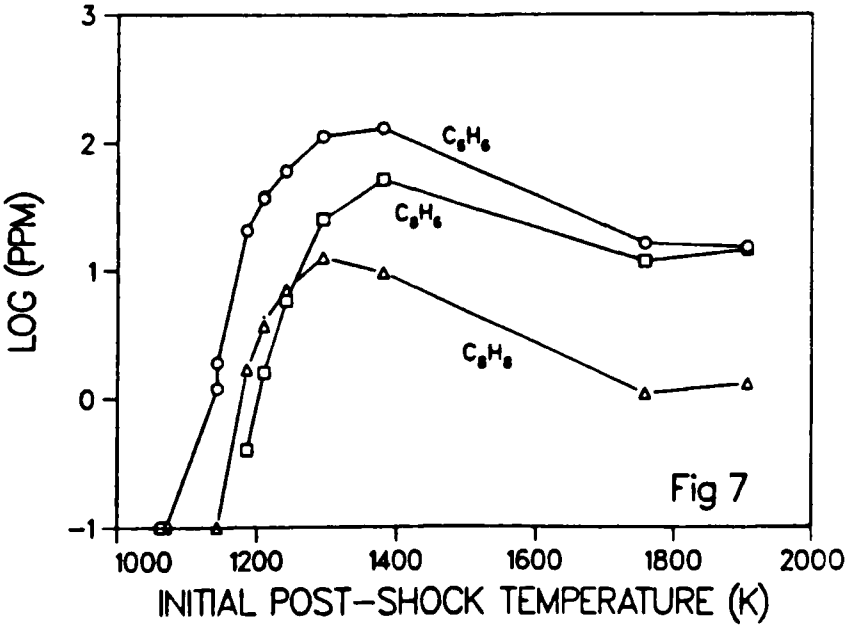

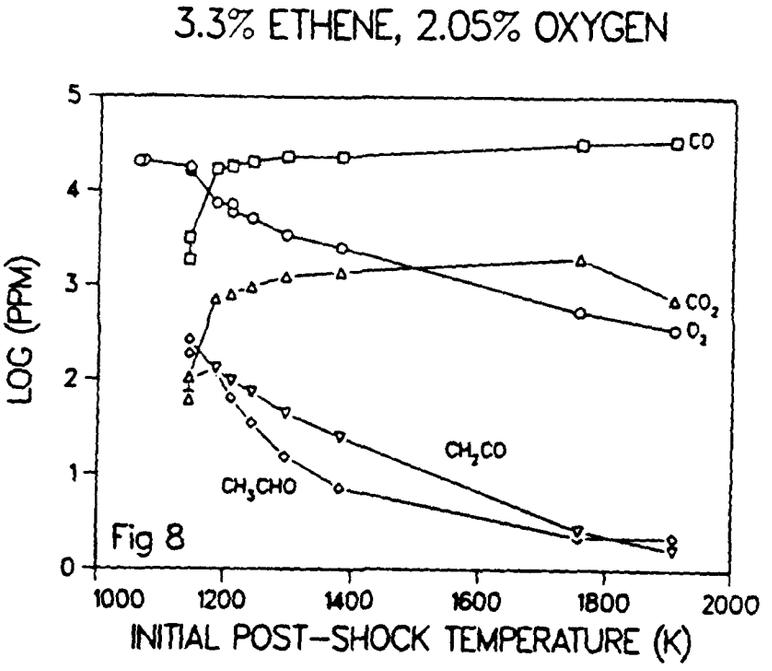
3.3% ETHENE, 2.05% OXYGEN
LOG (PPM)
INITIAL POST-SHOCK TEMPERATURE (K)
CO
CO_2
O_2
CH_2CO
CH_3CHO
Fig 8
0
1
2
3
4
5
1000
1200
1400
1600
1800
2000

APPENDIX I

THE PYROLYSIS OF ACETYLENE AND VINYLACETYLENE IN A SINGLE-PULSE SHOCK TUBE

Subject Matter:

1704 Kinetics
2401 Reaction Mechanisms
2701 Thermal Decomposition

Meredith B. Colket, III
United Technologies Research Center
Silver Lane, Mail Stop 30
East Hartford, CT 06108

accepted for presentation at

The Twenty-First International Symposium
on Combustion

to be held on
August 3-8, 1986

Munich, Germany

REVISED

Abstract

Acetylene and vinylacetylene have been pyrolyzed in a single-pulse shock tube for the temperature range 1100 to 2400 K, at total pressures of approximately eight atmospheres and for dwell times of approximately 700 microseconds. Initial concentrations of the hydrocarbon in argon ranged from about 100 ppm to 4%. Gas samples were collected and analyzed using gas chromatography for hydrogen, and C_1 to C_{10}-hydrocarbons. The data from the pyrolysis of acetylene exhibit substantial production of vinylacetylene, benzene, and phenylacetylene, but agree well with a detailed chemical kinetic model. Data from vinylacetylene pyrolysis and thermochemical arguments suggest a chain mechanism by which H adds to vinylacetylene and the resultant adduct decomposes to acetylene and a vinyl radical. Rate constants for the reverse steps of those occurring during vinylacetylene and benzene pyrolysis have been calculated using thermodynamics and forward rate constants. These reverse rate constants assist in describing the production of vinylacetylene, benzene, and phenylacetylene during acetylene pyrolysis.

Four separate reaction mechanisms for the initial formation of aromatic rings have been identified. The relative importance of each step depends on the ambient temperature and relative concentrations. Overall steps can be written as

$$C_2H_2 + n\text{-}C_4H_5 \rightarrow C_6H_6 + H$$

$$C_2H_2 + n\text{-}C_4H_3 \rightarrow C_6H_5$$

$$C_4H_4 + n\text{-}C_4H_5 \rightarrow C_6H_5C_2H_3 + H$$

$$C_4H_4 + C_2H_3 \rightarrow C_6H_6 + H$$

Introduction

Glassman[1] has convincingly argued that the chemistry of fuel pyrolysis plays an important role in sooting diffusion flames. Some pyrolysis steps may be rate-limiting for the production of incipient soot particles, and therefore the total amount of soot.[2] Armed with this information, many research programs have begun to identify the rate-limiting processes. For example, Bittner and Howard,[3] and Bockhorn, et al.[4] have provided experimental confirmation of a variety of high molecular weight polycyclic aromatics present in rich flames. Cole, et al.[5] and Weissman and Benson[6] have suggested mechanisms with rates consistent with thermochemical analysis and experimental data for the production of single-ring aromatics. Frenklach, et al.[7] has modeled soot formation from acetylene pyrolysis in shock tubes using a detailed chemical mechanism. The mechanism includes production of aromatic rings and continual growth of polycylic aromatics. Qualitative success has been obtained in this substantial effort despite the lack of confirming experimental data describing profiles of intermediates for confirmation/support of the proposed model.

It is the objective of the present work to extend these earlier works in order to help elucidate pyrolysis steps and chemical mechanisms related to the formation and break-up of aromatic rings. A single-pulse shock tube[8,9] was selected for this study, not only because shock tubes are one of the few devices capable of generating conditions of importance to soot formation in diffusion flames, but also to extend the information on soot production already generated through optical studies in shock tubes.[10-13]

Preliminary versions of the modeling work have been described separately for acetylene[14] and vinylacetylene.[15] The present work combines the earlier models, including a recent one for benzene pyrolysis,[16] into one model which satisfactorily describes both decomposition (of the parent hydrocarbons) and product formation. Required revisions include slight adjustments to rate constants and to assumed thermodynamic parameters.

Description of Facilities

The SPST used in this program is 285 cm long and has a diameter of 3.8 cm (i.d.). The driver is 88 cm in length and can be tuned by shortening its length in 3.8 cm increments; the driven section is 197 cm long. An 11.7 liter "dump tank" is located in the driver (lower pressure) section 30 cm downstream of the diaphragm. Pressure profiles were determined using Kistler pressure transducers located 15.25 and 2.50 cm from the end wall. Arrival times were measured to within one microsecond using digitized pressure traces. Calculated quench rates are typically 10^5 K/sec or higher in the rarefaction wave. Starting pressures prior to filling are 0.2μ and leak rates are less than 1μ/min. Post-shock temperatures were calculated based on the measured incident shock velocity and normal shock wave equations.

The procedures for performing an experiment are similar to those described by Tsang,[17] except for an automated sampling system. The sample is collected at the endwall of the shock tube using 0.045 inch i.d. tubing heated to over 85°C. Approximately 30 milliseconds after the gas has been shock heated and cooled, a solenoid valve opens to the evacuated sample cell and

then closes after 300 milliseconds. The sample storage vessel is all stainless steel with an internal volume of 25 cc.

The sampling volume is directly coupled to a low volume (<3cc), heated inlet system of a Hewlett Packard 5880 A gas chromatograph[14]. Valves, detectors and software integration routines as described previously[14] enable this system to provide automatic quantitative detection of hydrogen and hydrocarbon species up to C_{10}-hydrocarbons. Based on repeated injections of calibrated samples, overall accuracies are estimated to be three percent. Calibration gases were stored in stainless steel cylinders with degreased valves and were heated to approximately 60°C prior to injection.

Argon (99.999% pure) was obtained from Matheson and was the principal diluent. Compressed acetylene, also from Matheson, contained about 1 to 2% acetone (added for stability) depending on bottle conditions. Acetylene was purified by repeated freezing and thawing at liquid N_2 temperatures and retaining only the middle 50%. Final samples still contained 0.1 to 0.2% acetone. Vinylacetylene was obtained from Wiley Organics and contained an unidentified hydrocarbon with a concentration of approximately 8000 ppm.

Model Description

Detailed chemical kinetic calculations have been performed using CHEMKIN,[18] LSODE,[19] and a version of a shock tube code originally developed by Mitchell and Kee[20] but modified to include quenching effects in an SPST. Quenching rates are determined using experimental pressure traces, assuming adiabatic expansion, and using the equation

$$\frac{dT}{dt} = \frac{T}{P}\,\frac{\gamma-1}{\gamma}\,\frac{dP}{dt} \quad .$$

Calculated quenching rates vary as a function of shock strength and time. Initial quenching rates are as high as 2×10^6 K/sec for shocks producing initial post-shock temperatures of 2000°K, but only 25% of that rate for shocks producing reflected shock temperatures near 1200°K.

The chemical kinetic model used in this work is reproduced in Table I and is based on proposed mechanisms for the pyrolysis of acetylene[21] and ethene.[22] The reaction set includes the identification of the C_4H_3 isomers following Frenklach, et al.[7] The radicals are denoted n-C_4H_3 for the (normal) isomer with the unpaired electron on the terminal vinylic carbon and i-C_4H_3 for the (iso)isomer with the radical site on the interior carbon atom. n-C_4H_5 (radical on end carbon) was the only C_4H_5 isomer considered in this work. Also, the mechanism includes the forward and reverse processes of the predominant path for decomposition of benzene, i.e.,

$$C_6H_6+H \rightleftarrows C_6H_5+H_2$$

$$C_6H_5 \rightleftarrows \ell\text{-}C_6H_5$$

$$\ell\text{-}C_6H_5 \rightleftarrows n\text{-}C_4H_3+C_2H_2$$

where ℓ-C_6H_5 has been suggested[16] to be the 1-hexyne-^,5-dien-6-yl

radical. The rate constants (R55,R56) have been revised slightly from the previous work[16] in order to be consistent with the reverse processes.

As required, thermodynamic estimates of some species were made using group additivity techniques.[23] Otherwise, data from readily available sources were used.[24,25] Both estimates of rate parameters and those calculated using equilibrium constants are dependent on the selected thermodynamics. Of particular concern during the present research is the apparent uncertainty in the heat of formation of vinyl[26-27] and related (e.g. n-C_4H_3 and n-C_4H_5) radicals. Uncertainties in the heats of formation and entropies of these radicals directly translate into errors in proposed rate constants. Thermodynamic parameters at room temperature for species included in this work are presented in Table II.

Results and Discussion

Several series of runs of the pyrolysis of acetylene and vinylacetylene have been completed. Each series represents approximately 10 to 15 separate experiments and each experiment in a series has the same initial concentration in argon. For each run, a chemical analysis is performed of final product distribution. Initial post-shock temperatures for runs from a given series typically range from 1100 to 2400°K. Detailed chemical kinetic model calculations have been performed for most series and the numerical results for selected series are compared to the experimental data in Figs. 1,3-5. Mass balance data were presented previously.[14] A detailed discussion of the experimental data and kinetic mechanism follows.

Acetylene

The decomposition of 3.7% acetylene in argon and production of the major species, i.e. C_4H_2, H_2, and C_6H_2, agree well with existing kinetic models. As seen in Fig. 1, vinylacetylene (VA), benzene and phenylacetylene are also observed and may play a critical role in the growth and production of polycyclic aromatics. The bimolecular reaction $2C_2H_2 \rightarrow C_4H_4$ is thought to occur at low temperatures. Extrapolation of low temperature rate constants provided quantitative agreement with the experimental profile. In addition, the activation energy for this process (~40 kcal/mole) is in reasonable agreement with the assumption of intermediate formation of the C_4H_4 diradical, which is approximately 35 to 43 kcal more energetic than two molecules of acetylene.[28] Unfortunately, this mechanism does not provide a plausible, parallel path for the formation of benzene; yet the similarity in profiles of benzene and VA strongly suggest a parallel mechanism. Stein[29] suggested an alternative chain process initiated by H-atom addition to acetylene to form VA, i.e.,

$$C_2H_2(+H) \rightarrow C_2H_3(+C_2H_2) \rightarrow n\text{-}C_4H_5(-H) \rightarrow C_4H_4$$

This sequence is identical to the first steps in the ring formation process proposed by Frenklach, et al.[7] The final steps of the proposed process include

$$C_4H_4(-H) \rightarrow n\text{-}C_4H_3(+C_2H_2) \rightarrow \ell\text{-}C_6H_5 \rightarrow \text{phenyl}$$

followed by subsequent formation of benzene or phenylacetylene.

Detailed chemical kinetic modeling of the present experimental data, however, strongly suggests that early (i.e. low temperature) benzene formation arises principally from acetylene addition to the normal-butadienyl radical, not the n-C_4H_3 radical, i.e.,

$$n\text{-}C_4H_5(+C_2H_2) \rightarrow \ell\text{-}C_6H_7 \rightarrow c\text{-}C_6H_7(-H) \rightarrow C_6H_6$$

where ℓ-C_6H_7 is defined to be the 1,3,5-hexatrien-1-yl radical. Preliminary calculations using this mechanism have also been performed for comparison to the flow reactor data on acetylene pyrolysis obtained by Munson and Anderson.[30] Semi-quantitative agreement for the production of benzene and VA was achieved and thus the bimolecular reaction involving intermediate formation of a C_4H_4 diradical is not necessary to describe lower temperature acetylene pyrolysis.

Above 1500°K, cyclic compounds are formed principally by acetylene addition to n-C_4H_3 in agreement with the proposal by Frenklach, et al.[7] Previously it was assumed, however, that n-C_4H_3 was formed through path A, whereas (R-12) was the dominate route under the present conditions

$$n\text{-}C_4H_5(-H) \rightarrow C_4H_4(-H) \rightarrow n\text{-}C_4H_3 \qquad A$$

$$C_2H_2 + C_2H \rightarrow n\text{-}C_4H_3 \qquad (-12)$$

This conclusion arises from results discussed later in this paper which show that VA decomposition principally involves H-atom addition to C_4H_4, not H-atom abstraction. As temperature increases, the abstraction route will become more significant; however, the concentration of C_2H will also increase so (R-12) still remains competitive. Furthermore (R-12) is a straightforward process for producing the normal radical and, in Figure 1, assists in adequately describing the production of benzene and phenylacetylene. Demonstration of the relative sources of n-C_4H_3 can be seen in Figure 2, where reaction sources and sinks are plotted as a function of time for two different temperatures.

Figure 1 shows that the model overpredicts observed benzene and phenylacetylene concentrations above 1600°K. Coincidentally, this is the same temperature at which a significant deficit in recovered mass first appears.[14] Some phenylacetylene and benzene above 1600°K is probably converted to higher molecular weight species which are not observed and not accounted for by the model.

Vinylacetylene

Mixtures of 0.01, 0.115 and 1.0% VA in argon were pyrolyzed over the temperature range 1100 to 2500°K. The data for the lowest and highest concentrations are presented in Figs. 3, 4 and 5. The other species not shown in these figures were observed at concentrations less than 2% of the parent. These species include methane, ethylene, allene/methylacetylene, several unidentified C_5 species, C_6H_4, toluene, and a C_9-hydrocarbon (possibly indene). Data on the series with intermediate concentration have been presented previously.[15] The most significant information is that at low

temperatures and low initial concentrations, acetylene is the predominant product, while diacetylene (as well as H_2) is produced at levels approximately ten times less than that of acetylene. Aromatics are produced at higher temperaures and concentrations, but not in quantities sufficient to encourage rapid growth of polycylics and severe mass imbalance. Relatively little data[31] have been presented previously for comparison to this SPST data. Lundgard's review has identified one previous work[32] which overlaps the present temperature range. Yampol'skii, et al. examined VA pyrolysis between 1023 and 1273°K and produced qualitatively similar results to the SPST work. The main low temperature aliphatic found by Yampol'skii was acetylene with traces of methane and ethene, although diacetylene was not detected. Benzene was also observed previously, as well as a polymer whose precursor may be styrene. The overall decomposition of VA observed by Yampol'skii, et al., $k=1.6\times10^{11}$ exp (-52,800cal/RT) sec^{-1} is approximately five times higher than the SPST results.

Kinetic modeling requires the identification of the initiation step and a chain process which describes the predominant formation of acetylene with minor production of diacetylene, styrene, benzene and phenylacetylene. The three possible initiation processes are

R9 $C_4H_4 \rightarrow i\text{-}C_4H_3 + H$ - 98 kcal/mole

R10 $C_4H_4 \rightarrow n\text{-}C_4H_3 + H$ -111 kcal/mole

R51 $C_4H_4 \rightarrow C_2H+C_2H_3$ -122 kcal/mole

where the estimated endothermicities may each be in error by as much as 10 kcal/mole due to uncertainties in heats of formation of the hydrocarbon radicals. In this work, the principal initiation process was assumed to be Reaction 9, which required a rate expression of $10^{15.2}$ exp (-42800/T) sec^{-1}, although the A-factor seems high and E_{act}, low, for the C-H bond scission. It is important to note that the model results were relatively insensitive to the absolute magnitude of the initiation rate or its temperature dependence. A factor of three change in the initiation rate resulted in approximately a 20-30% change in the overall rate of decomposition and the formation of products. The explanation for this phenomenon is that the decomposition of VA in the range 1200-1400°K is controlled by a chain mechanism:

			$\log_{10}A$	E_{act}
R9	initiation	$C_4H_4 \rightleftarrows i\text{-}C_4H_3+H$	15.2	85000.
R-46	chain	$H+C_4H_4 \rightleftarrows n\text{-}C_4H_5$	13.0	1370.
R-20	chain	$n\text{-}C_4H_5 \rightleftarrows C_2H_3+C_2H_2$	14.0	43360.
R-3	chain	$C_2H_3 \rightleftarrows H+C_2H_2$	13.0 cc,mole,sec	43710. cal/mole

where the last three reactions account for the majority of the decomposition of the parent and the predominance of acetylene in the low-temperature products. This chain is not only important specifically to understanding the

pyrolysis of vinylacetylene; but, as discussed earlier in this paper, also to the mechanism of ring formation during acetylene pyrolysis. Explanations for elimination of other mechanisms is presented below.

Alternative chain mechanisms for decomposition of VA would include H-atom abstraction from C_4H_4 resulting in $\dot{C}:CCH:CH_2$, $CH:C\dot{C}:CH_2$, or $CH:CCH:\dot{C}H$. Formation of the first of these can be neglected from thermodynamic considerations. In addition, direct formation of two acetylene molecules from this structure seems unlikely. The second isomer, i-C_4H_3, should decompose principally into diacetylene, since breakage of the C-C bond would have a high activation barrier due to the formation of vinylidene as an intermediate. The last isomer, n-C_4H_3, may decompose into C_4H_2+H or C_2H+C_2H_2. Estimated rates

		Log k(1300°K)	$Log_{10}A$	E
R12	n-C_4H_3 ⇄ C_2H+C_2H_2	4.72	14.3	57000.
R14	n-C_4H_3 ⇄ C_4H_2+H	5.88	12.6	40000.

suggest that Reaction 14, i.e. production of C_4H_2, is faster by a factor of 14 near 1300°K where VA decomposition is observed. At higher temperatures the two rates approach one another. These relative rate estimates are supported by experimental decomposition data of benzene pyrolysis from Kern, et al.[33] Those researchers found that the initial ratio of products C_2H_2/C_4H_2 at 1700°K, is approximately two to one. Assuming the overall decomposition path

$$C_6H_6(-H) \rightleftarrows C_6H_5 \rightleftarrows n\text{-}C_4H_3+C_2H_2,$$

then the C_2H_2/C_4H_2 product ratio suggests that the branching ratio k_{14}/k_{12} is also approximately two to one. The calculated ratio using the above rates is three (3) at 1700°K. Thus, if n-C_4H_3 is the principal intermediate from VA decomposition, then the initial production rate of C_4H_2 would be similar to or higher than that of C_2H_2 during VA pyrolysis. Such a prediction is not substantiated by the SPST experiments.

H-atoms may add to VA at locations other than to the secondary acetylenic carbon. Addition to the other carbons would form $H_2C:\dot{C}CHCH_2$, $HC:\dot{C}CHCH_3$, or $HC:CCH_2\dot{C}H_2$. However, each of these radicals would be expected to reform VA, decompose into products other than two acetylenes or involve energetic intermediates. Thus it appears that the decomposition chain involving n-C_4H_5 will dominate. Detailed chemical kinetic calculations using the specific rate constants in Table I are consistent with this analysis.

Production of diacetylene is described by

$$R+C_4H_4 \rightarrow i\text{-}C_4H_3+RH$$

$$R+C_4H_4 \rightarrow n\text{-}C_4H_3+RH$$

followed by decomposition of C_4H_3 into diacetylene plus H-atoms. R may be an H-atom or a hydrocarbon radical.

As shown in Fig. 5, reasonable agreement with experimental profiles of aromatic species were obtained using the reaction sequence of Table I. The apparent underprediction of VA at elevated temperatures is presumably an experimental problem due to partial gas sampling of boundary layers which contain the unheated parent hydrocarbon. Above 1600°K, phenyl is formed from the $n\text{-}C_4H_3+C_2H_2$ recombination and is followed by conversion to benzene or phenylacetylene. At lower temperatures, the predominate formation routes of aromatics are

R45 $C_4H_4+C_2H_3 \rightarrow C_6H_7$ (1,3,5-hexatrien-3-yl)

$C_6H_7 \rightarrow c\text{-}C_6H_7$

$c\text{-}C_6H_7 \rightarrow C_6H_6+H$

for benzene formation, and

R52 $C_4H_4+n\text{-}C_4H_5 \rightarrow C_8H_9$

$C_8H_9 \rightarrow c\text{-}C_8H_9$

$c\text{-}C_8H_9 \rightarrow C_8H_8+H$

to produce styrene. PA is produced principally by

R53 $C_8H_8+H \rightarrow C_8H_7+H_2$

$C_8H_7 \rightarrow C_8H_6+H$

near 1500°K and below, but at higher temperatures, acetylene addition to phenyl also occurs. Reactions 45, 52, and 53 were assumed to be overall processes and nonreversible. For the conditions (radical concentrations and temperatures) at which these reactions contribute, preliminary calculations confirmed the validity of these assumptions. Despite the good agreement with the experimental data, there are several unsettling features of these proposals. Reaction 45 requires a 1,3 or 1,4 H-atom shift prior to cyclization and Reaction 47, which has been proposed previously[5] should be a preferred route for aromatization. However, $k_{47} \approx 10^{14}$ cc/mole-sec would be required to explain the experimental data. This rate is significantly higher than the rate in Table I, 2×10^{11} cc/mole-sec, required by the acetylene modeling and previous determinations [7.5×10^{10} (Ref. 5) and 2.7×10^{11} (Ref. 6) at 1300°K].

Another concern of the modeling results is that the value of k_{52} required to match the experimental data is approximately 100 times higher than a previous determination using data from a low pressure, premixed butadiene flame. Rate determinations from the SPST data are subject to errors due to boundary-layers, quenching effects, and modeling complexity. However, the flame determination is expected to be a lower limit since, when evaluating the rate constant, Cole, et al.[5] assumed that the $n\text{-}C_4H_5$ radical was the dominant C_4H_5 species. Other isomers, particularly $H_2C{:}CH\dot{C}CH_2$, which is less reactive and more stable by 3 kcal/mole, can contribute significantly to mass 53.

The assumption of the predominance of n-C_4H_5 in the flame work would only partially explain the difference between the two evaluations. Uncertainties in heats of formation and entropies for n-C_4H_5 and/or vinyl, which may affect the n-C_4H_5 concentration via

$$C_2H_2+C_2H_3 \rightleftarrows n\text{-}C_4H_5$$

may also help to alleviate the difference; but probably by no more than a factor of five. Alternatively, reactions not considered in the present work may describe production of aromatics or significantly enhance the concentration of n-C_4H_5.

Conclusions

Single-pulse shock tube data have been obtained for the pyrolyses of acetylene and vinylacetylene. The data have been used to support previous proposals for acetylene and benzene pyrolysis with some revisions. A decomposition model for vinylacetylene involving H-atom addition to vinylacetylene has been proposed in order to explain product formation. Severe constraints imposed by simultaneously modeling decomposition of each of the parent hydrocarbons as well as five or more product species have been satisfied with the proposed model. Vinylacetylene, benzene, and phenylacetylene are observed during acetylene pyrolysis. The sequence

$$C_2H_2+H \rightleftarrows C_2H_3$$

$$C_2H_2+C_2H_3 \rightleftarrows n\text{-}C_4H_5$$

$$n\text{-}C_4H_5 \rightleftarrows C_4H_4+H$$

$$C_2H_2+n\text{-}C_4H_5 \rightarrow \ell\text{-}C_6H_7 \text{ (1,3,5-hexatrien-1-yl)}$$

$$\ell\text{-}C_6H_7 \rightarrow c\text{-}C_6H_7$$

$$c\text{-}C_6H_7 \rightarrow C_6H_6+H$$

describes the low temperature formation of vinylacetylene and benzene (1100-1400°K). Reverse rates calculated from thermodynamics for the first three steps describe the decomposition of vinylacetylene. At temperatures above 1500°K, phenyl is formed by

$$C_2H_2+H \rightleftarrows C_2H+H_2$$

$$C_2H_2+C_2H \rightleftarrows n\text{-}C_4H_3$$

$$C_2H_2+n\text{-}C_4H_3 \rightleftarrows \ell\text{-}C_6H_5 \text{ (1-hexyne-3,5-dien-6-yl)}$$

$$\ell\text{-}C_6H_5 \rightleftarrows \text{phenyl}$$

and is followed by formation of benzene or phenylacetylene. Reverse rates calculated from thermodynamics are consistent with a previous proposal for decomposition of phenyl during benzene pyrolysis.

Aromatic formation during vinylacetylene pyrolysis at low temperatures is described by

$$C_2H_3+C_4H_4 \rightarrow C_6H_7 \text{ (1,3,5-hexatrien-3-yl)}$$

$$C_6H_7 \rightarrow c\text{-}C_6H_7$$

$$c\text{-}C_6H_7 \rightarrow C_6H_6+H$$

$$\text{and } n\text{-}C_4H_5+C_4H_4 \rightarrow \ell\text{-}C_8H_9$$

$$\ell\text{-}C_8H_9 \rightarrow c\text{-}C_8H_9$$

$$c\text{-}C_8H_9 \rightarrow C_8H_8+H$$

The proposed rate constant for the first step is low, but the reaction requires an H-atom shift. The required rate for the addition of the normal butandienyl radical to vinylacetylene is approximately 100 times higher than a previous measurement. Consequently, it is possible that calculated concentrations of $n\text{-}C_4H_5$ are inaccurate or that other mechanisms are significant.

Acknowledgements

This work has been supported in part by the Air Force Office of Scientific Research (AFSC) under Contract No. F49620-85-C-0012. The United States government is authorized to reproduce and distribute reprints for governmental purposes, notwithstanding any copyright notation herein. The author is indebted to Dr. D. J. Seery for his constant support and suggestions throughout this research. The author is also grateful to Dr. P. R. Westmoreland for many fertile discussions and his sharing of technical/thermodynamic information. The authors of CHEMKIN and LSODE should be acknowledged, since these computer routines substantially increased the capability for performing the model calculations; particular thanks should go to Dr. R. J. Kee for his suggestions and guidance in modifying the codes. The experimental research has been completed only with the able assistance of D. Kocum. His assistance is greatly appreciated.

References

1. Glassman, I.: "Phenomenological Models of Soot Processes in Combustion Systems," Department of Mechanical and Aerospace Engineering Report 1450, Princeton University, NJ (1979).

2. Harris, S.J. and Weiner, A.M.: Combustion Science and Technology, 31, 155 (1983). Also 32, 267 (1983).

3. Bittner, J. and Howard, J.B.: Eighteenth Symposium (International) on Combustion, p. 1105, The Combustion Institute, Pittsburgh (1981).

4. Bockhorn, H., Fetting, F. and Wenz, H.W.: Ber.Bunsenges.Phys.Chem., 87, 1067 (1983).

5. Cole, J.A., Bittner, J.D., Longwell, J.P. and Howard, J.B.: Combustion and Flame, 56, 51 (1984).

6. Weissman, M. and Benson, S.W.: Int'l.J.Chem.Kin., 16, 307 (1984).

7. Frenklach, M., Clary, D.W., Gardiner W.C., Jr., and Stein, S.: Twentieth Symposium (International) on Combustion, p. 887, The Combustion Institute, Pittsburgh (1985).

8. Glick, H.S., Squire, W., and Hertzberg, A.: Fifth Symposium (International) on Combustion, p. 393, Reinhold Publishing Corp., New York, (1955).

9. Lifshitz, A., Carroll, H.F. and Bauer, S.H.: J.Chem.Phys., 39, pp. 1661-1665 (1963).

10. Graham, S.C., Homer, J.B. and Rosenfeld, J.L.J.: Proc.R.Soc.London A344,259 (1975).

11. Wang, T.S., Matula R.A., and Farmer, R.C.: Eighteenth Symposium (International) on Combustion, p. 1149-1158, The Combustion Institute, Pittsburgh (1981).

12. Frenklach, M., Ramachandra, M.K. and Matula, R.A.: Twentieth Symposium (International) on Combustion, p. 871, The Combustion Institute, (1984).

13. Rawlins, W.T., Cowles, L.M. and Krech, R.H.: Twentieth Symposium (International) on Combustion, p. 879, The Combustion Institute, (1985).

14. Colket, M.B.: To be published in Shock Tubes and Waves, Proceedings of the Fifteenth International Symposium (1986).

15. Colket, M.B.: "Pyrolysis of Vinylacetylene," Paper No. 53, presented at Eastern Section/Combustion Institute, Fall Technical Meeting, Philadelphia, November 1985.

16. Colket, M.B.: "Pyrolysis of C_6H_6" presented at American Chemical Society, New York City National Meeting, Division of Fuel Chemistry preprints 31 (2), p. 98, April 13-16, 1986.

17. Tsang, W.: Shock Waves in Chemistry, Ed. by A. Lifshitz, Marcel Dekker, Inc., New York, pp. 59-129 (1981).

18. Kee, R.J., Miller J.A. and Jefferson, T.H.: "CHEMKIN: A General-Purpose, Problem-Independent, Transportable, Fortran Chemical Kinetics Code Package," Sandia National Labortories, SAND80-8003, March 1980.

19. Hindmarsh, A.C.: "LSODE and LSODI, Two New Initial Value Differential Equation Solvrs," ACM SIGNUM Newsletter, 15, No. 4, Dec. 1980.

20. Mitchell, R.E. and Kee, R. J.: "A General-Purpose Computer Code for Predicting Chemical Kinetic Behavior behind Incident and Reflected Shocks," Sandia National Laboratories, SAND82-8205, March 1982.

21. Tanzawa, T. and Gardiner, W.C., Jr.: Combust. Flame 39, 241 (1980), also J.Phys.Chem. 84, 236 (1980).

22. Kiefer, J.H., Kapsalis, S.A., Al-Alami, M.Z., and Budach, K.A.: Combust. Flame 51, 79 (1983).

23. Benson, S.W.: Thermochemical Kinetics, J. Wiley and Sons, New York (1976).

24. Stull, D.R. and Prophet, H., JANAF Thermochemical Tables, 2nd Ed., U.S. Dept. of Commerce, Nat.Bur.Stand., Washington, D.C. (1971).

25. Burcat, A.: in Combustion Chemistry, p. 457, ed. by Gardiner, W.C., Springer-Verlag, New York (1984).

26. Kiefer, J.H., Wei, H.C., Kern, R.D. and Wu, C.H.: Int.J.Chem.Kin. 17, 225 (1985).

27. Sharma, R.B., Serno, N.M. and Koski, W.S.: Int.J.Chem.Kin. 17, 831 (1985).

28. Kollmar, H., Carrion, F., Dewar, M.J.S., and Bingham, R.C.: J.American Chemical Society 103, 5292, 1981.

29. Stein, S.E.: private communication (1984).

30. Munson, M.S.B. and Anderson, R.C.: Carbon 1, 51 (1963).

31. Lundgard, R.A.: "The Pyrolysis of Vinylacetylene," Ph.D. Thesis, Pennsylvania State University, available from University Microfilms International, Ann Arbor, Michigan (1983).

32. Yampol'skii, Yu. P., Maksimov, Yu V., and Lavroskii, K.P.: J.Phys.Chem. USSR (English translation) 182, 940 (1968).

33. Kern, R.D., Wu, C.H., Skinner, G.B., Rao, U.S., Kiefer, J.H., Towers, J.A., and Mizerka, L.J.: Twentieth Symposium (International) on Combustion, The Combustion Institute, p. 789 (1984).

34. Kiefer, J.H., Mizerka, L.J., Patel, M.R., and Wei, H.-C., J.Phys.Chem. 89, 2013 (1985).

35. Ebert, K.H., Ederer, H.J. and Isbarn, G.: Int.J.Chem.Kin. 15, 475 (1983).

36. Miller, J.A., Mitchell, R.E., Smooke, M.D. and Kee, R.J.: Nineteenth Symposium (International) on Combustion, The Combustion Institute, p. 181 (1982).

37. Fujii, N. and Asaba, T.: Fourteenth Symposium (International) on Combustion, The Combustion Institute, Pittsburgh, p. 433 (1973).

38. Mallard, W.G., Fahr, A., and Stein, S.E.: "Rate Constants for Phenyl Reactions with Ethylene and Acetylene," Paper No. 92, Chem.Phys.Proc. Comb., ES/CI, Clearwater Beach, Fla., Dec. 3-5, 1984.

TABLE I

PROPOSED SET OF REACTIONS AND RATE COEFFICIENTS

$\log k = \log A + n \log T - E/R/T/2.303$ *

	Reactions	Forward Rate Constant			Reverse Rate Constant			
		logA	n	E	logA	n	E	Ref
1	C2H4+M=C2H3+H+M	16.16	0.0	81.8	14.24	0.0	-23.0	22
2	C2H4+H=C2H3+H2	14.84	0.0	14.5	13.53	0.0	14.0	21
3	H+C2H2=C2H3	12.74	0.0	2.5	13.01	0.0	43.8	21
4	C2H3+H=H2+C2H2	13.00	0.0	0.0	13.34	0.0	63.2	21
5	H2+M=2H+M	12.35	-.5	92.5	11.74	-.5	-11.9	21
6	C2H2+M=C2H+H+M	16.62	0.0	107.0	15.25	0.0	-17.9	21
7	2C2H2=n-C4H3+H	12.30	0.0	45.9	11.67	0.0	-25.0	21
8	i-C4H3+H2=C2H2+C2H3	10.70	0.0	20.0	11.41	0.0	17.1	PW*
9	C4H4=i-C4H3+H	15.20	0.0	85.0	12.72	0.0	-12.1	PW
10	C4H4=n-C4H3+H	15.00	0.0	100.0	12.93	0.0	-7.7	PW
11	C2H+C4H4=C2H2+i-C4H3	13.60	0.0	0.0	12.48	0.0	27.9	21
12	n-C4H3=C2H2+C2H	14.30	0.0	57.0	13.56	0.0	3.0	PW
13	i-C4H3=C4H2+H	12.00	0.0	49.0	12.86	0.0	-0.2	PW
14	n-C4H3=C4H2+H	12.60	0.0	40.0	13.04	0.0	1.4	PW
15	n-C4H3+H=i-C4H3+H	13.48	0.0	0.0	13.06	0.0	10.7	PW
16	i-C4H3+H=C4H2+H2	13.00	0.0	0.0	14.47	0.0	55.2	PW
17	n-C4H3+H=C4H2+H2	13.00	0.0	0.0	14.05	0.0	65.9	PW
18	C4H4+H=i-C4H3+H2	14.49	0.0	14.5	12.62	0.0	21.9	26,PW
19	C4H4+H=n-C4H3+H2	13.90	0.0	14.5	12.45	0.0	11.2	26,PW
20	C2H3+C2H2=n-C4H5	12.04	0.0	4.0	13.79	0.0	37.7	PW
21	C2H+H2=H+C2H2	12.85	0.0	0.0	13.60	0.0	20.5	22
22	C2H+C2H2=C4H2+H	13.60	0.0	0.0	14.78	0.0	15.4	21
23	C4H2=C4H+H	14.89	0.0	120.0	13.28	0.0	2.1	22
24	C2H+C4H2=C6H2+H	13.60	0.0	0.0	14.97	0.0	15.1	21
25	C4H+C2H2=C6H2+H	13.30	0.0	0.0	14.91	0.0	8.1	21,PW
26	C6H2=C6H+H	14.89	0.0	120.0	13.05	0.0	5.3	22
27	C4H+H2=H+C4H2	13.30	0.0	0.0	14.30	0.0	13.5	22
28	C6H+H2=H+C6H2	13.30	0.0	0.0	14.53	0.0	10.3	22
29	C2H+H=C2+H2	12.00	0.0	23.0	11.55	0.0	3.8	PW
30	C2H+M=C2+H+M	16.67	0.0	124.0	15.61	0.0	0.4	36
31	C4H4+C6H5=C6H6+n-C4H3	12.00	0.0	0.0	12.56	0.0	3.1	PW
32	C4H4+C6H5=C6H6+i-C4H3	12.00	0.0	0.0	12.14	0.0	13.8	PW

* NOTES: Units for A: cc,moles,sec.
Units for E: kcal/mole.
"=" represents forward and reverse directions included in model.
"-" represents forward direction only included in model.
PW indicates rate evaluted from the present work.

CONTINUED ON NEXT PAGE

TABLE I (continued)
PROPOSED SET OF REACTIONS AND RATE COEFFICIENTS
$\log k = \log A + n \log T - E/R/T/2.303$ *

	Reactions	Forward Rate Constant			Reverse Rate Constant			
		logA	n	E	logA	n	E	Ref
33	C2H+C6H6=C6H5+C2H2	13.30	0.0	0.0	12.05	0.0	14.1	34
34	C4H+C6H6=C6H5+C4H2	13.30	0.0	0.0	12.29	0.0	7.0	34
35	C2H3+C4H2=C4H4+C2H	13.48	0.0	23.0	13.46	0.0	3.1	PW*
36	C2H3+C4H4=C2H4+n-C4H3	11.70	0.0	16.3	11.55	0.0	13.4	35,PW
37	C2H3+C4H4=C2H4+i-C4H3	11.70	0.0	16.3	11.13	0.0	24.1	35,PW
38	C6H6=C6H5+H	16.18	0.0	107.9	13.55	0.0	-3.0	16
39	C6H6+H=C6H5+H2	14.40	0.0	16.0	12.39	0.0	9.5	34
40	2C6H5=C12H10	12.48	0.0	0.0	16.57	0.0	108.3	17
41	C6H5+C6H6=C12H10+H	11.80	0.0	11.0	13.27	0.0	8.4	37
42	n-C4H3+C6H5-C10H8	13.00	0.0	0.0	0.00	0.0	0.0	PW
43	C2H2+C6H5=C8H6+H	12.00	0.0	4.0	13.50	0.0	3.1	38,PW
44	C2H4+C6H5=C8H8+H	11.57	0.0	2.1	12.99	0.0	1.6	38
45	C2H3+C4H4-C6H6+H	11.60	0.0	0.0	0.00	0.0	0.0	PW
46	n-C4H5=C4H4+H	14.00	0.0	41.4	13.42	0.0	3.2	6
47	n-C4H5+C2H2=1-C6H7	12.81	0.0	9.0	14.80	0.0	44.4	6,PW
48	n-C4H5+H=C4H4+H2	13.00	0.0	0.0	13.03	0.0	66.2	PW
49	C4H6+H=n-C4H5+H2	14.00	0.0	14.5	12.80	0.0	11.2	26,PW
50	C6H6+C2H=C8H6+H	12.00	0.0	0.0	12.25	0.0	13.2	PW
51	C4H4=C2H+C2H3	16.00	0.0	105.0	13.46	0.0	-15.5	PW
52	C4H4+n-C4H5-C8H8+H	13.90	0.0	3.0	0.00	0.0	0.0	PW
53	C8H8+H-C8H6+H+H2	14.60	0.0	7.0	0.00	0.0	0.0	PW
54	C6H5+C2H3=C8H8	13.00	0.0	0.0	16.34	0.0	104.4	PW
55	1-C6H5=n-C4H3+C2H2	14.00	0.0	36.0	11.71	0.0	-0.1	PW
56	C6H5=1-C6H5	13.54	0.0	65.0	10.22	0.0	1.4	PW
57	C6H6+H=c-C6H7	13.60	0.0	4.3	13.12	0.0	24.6	PW
58	c-C6H7=1-C6H7	14.48	0.0	50.0	11.36	0.0	0.4	PW

* NOTES: Units for A: cc,moles,sec.
Units for E: kcal/mole.
"=" represents forward and reverse directions included in model.
"-" represents forward direction only included in model.
PW indicates rate evaluted from the present work.

TABLE II

Selected Thermodynamics at 300K

Species	Heat of Formation (kcal/mole)	Entropy
$C_{12}H_{10}$	43.6	93.7
$C_{10}H_8$	36.0	79.5
C_8H_6	78.3	79.6
ℓ-C_6H_7	97.4	81.8
c-C_6H_7	49.9	72.1
C_6H_6	19.9	65.2
C_6H_5	78.5	69.4
ℓ-C_6H_5	139.2	80.0
C_6H_2	169.7	71.1
C_6H	233.2	74.3
C_4H_6	26.1	66.6
n-C_4H_5	82.5	69.1
C_4H_4	69.4	66.1
n-C_4H_3	125.1	68.7
i-C_4H_3	115.2	71.6
C_4H_2	111.7	59.9
C_4H	179.0	62.8
C_2H_4	12.6	52.4
C_2H_3	65.7	54.5
C_2H_2	54.2	48.1
C_2H	128.5	49.6
C_2	200.2	47.7

LIST OF FIGURES

Fig. 1

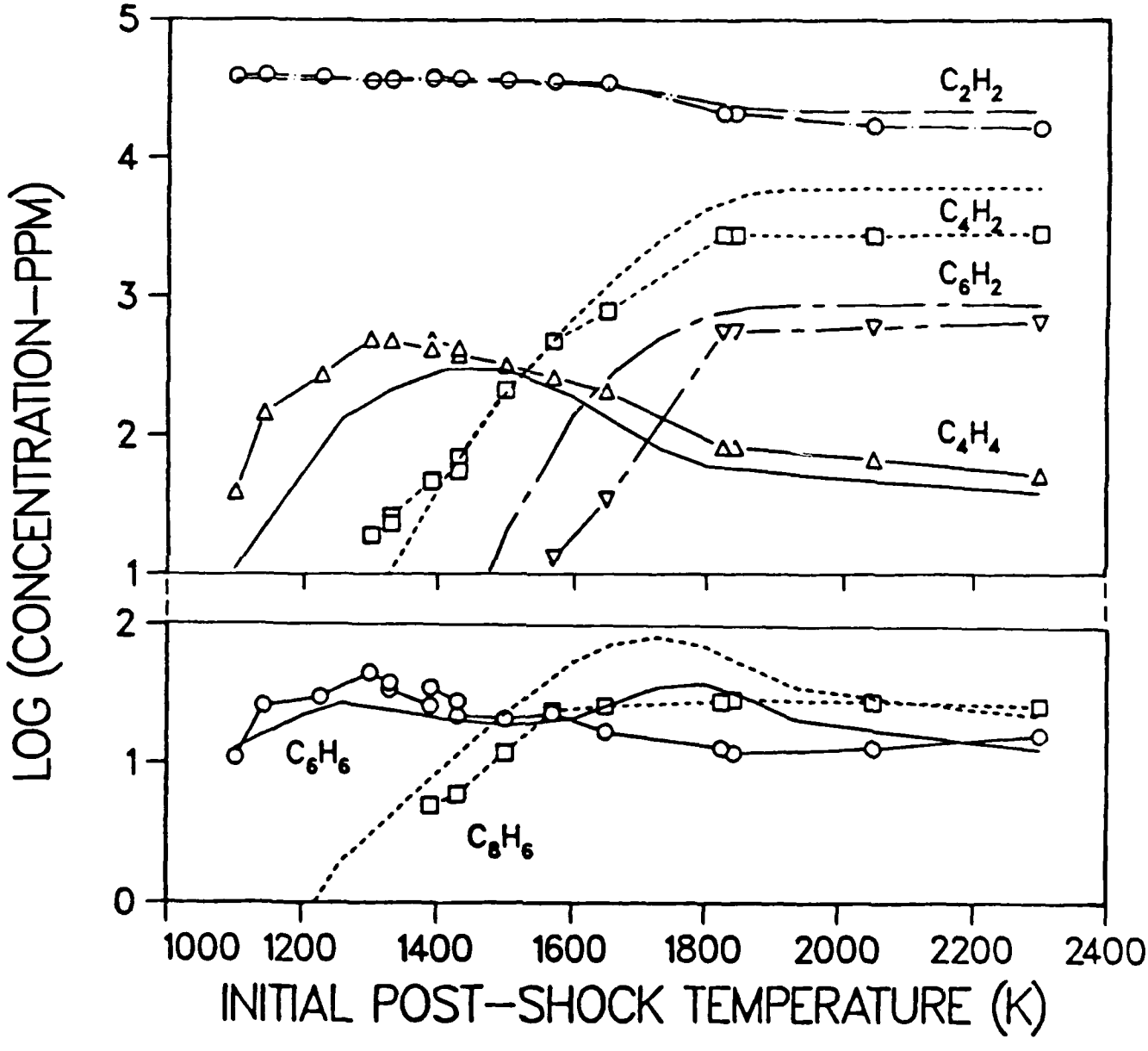
LOG (CONCENTRATION–PPM)
INITIAL POST–SHOCK TEMPERATURE (K)
C_2H_2
C_4H_2
C_6H_2
C_4H_4
C_6H_6
C_8H_6
5
4
3
2
1
2
1
0
1000
1200
1400
1600
1800
2000
2200
2400

Fig. 2a

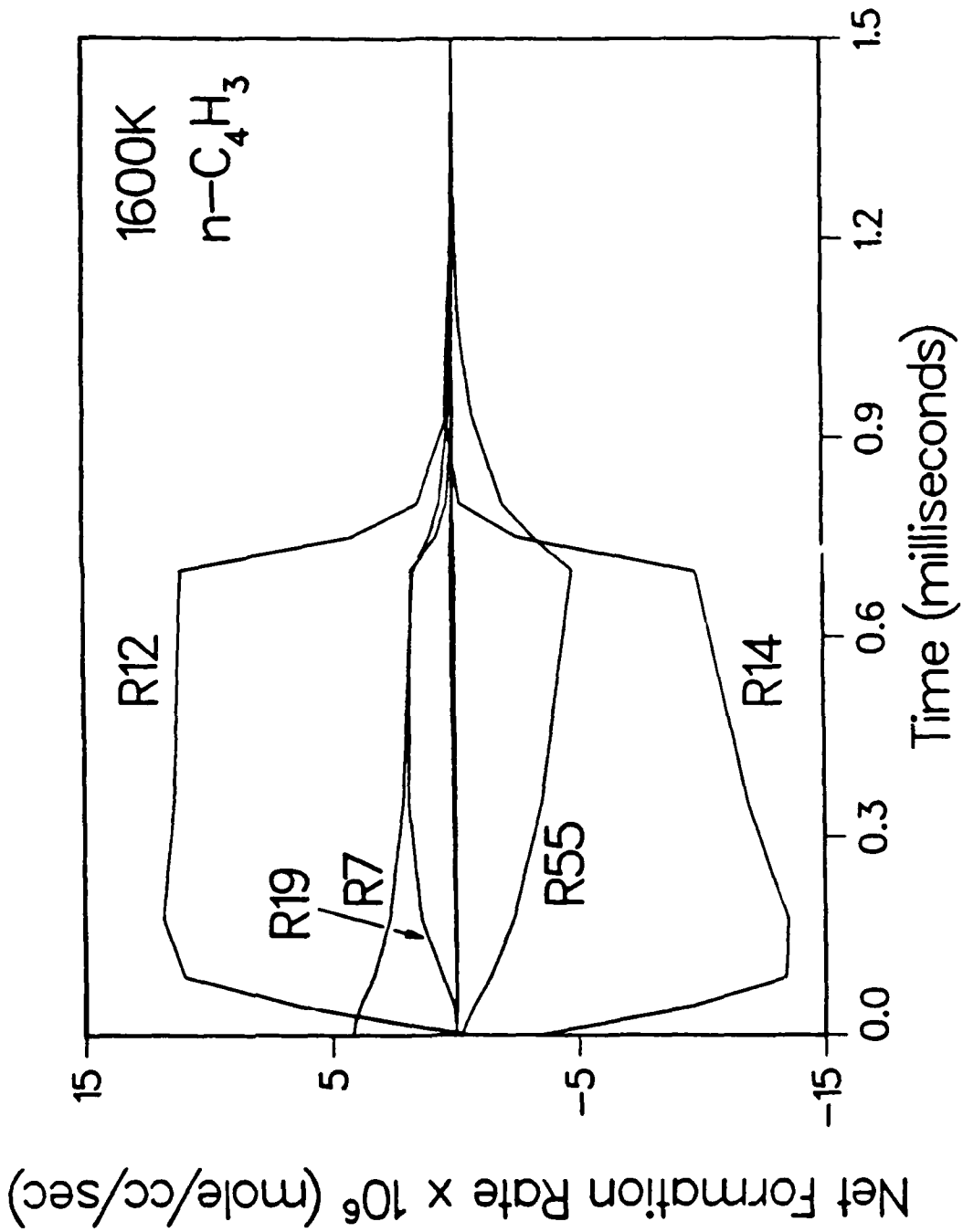
1600K
n−C4H3
R12
R19
R7
R55
R14
15
5
−5
−15
0.0
0.3
0.6
0.9
1.2
1.5
Time (milliseconds)
Net Formation Rate x 10⁶ (mole/cc/sec)

Fig. 2b

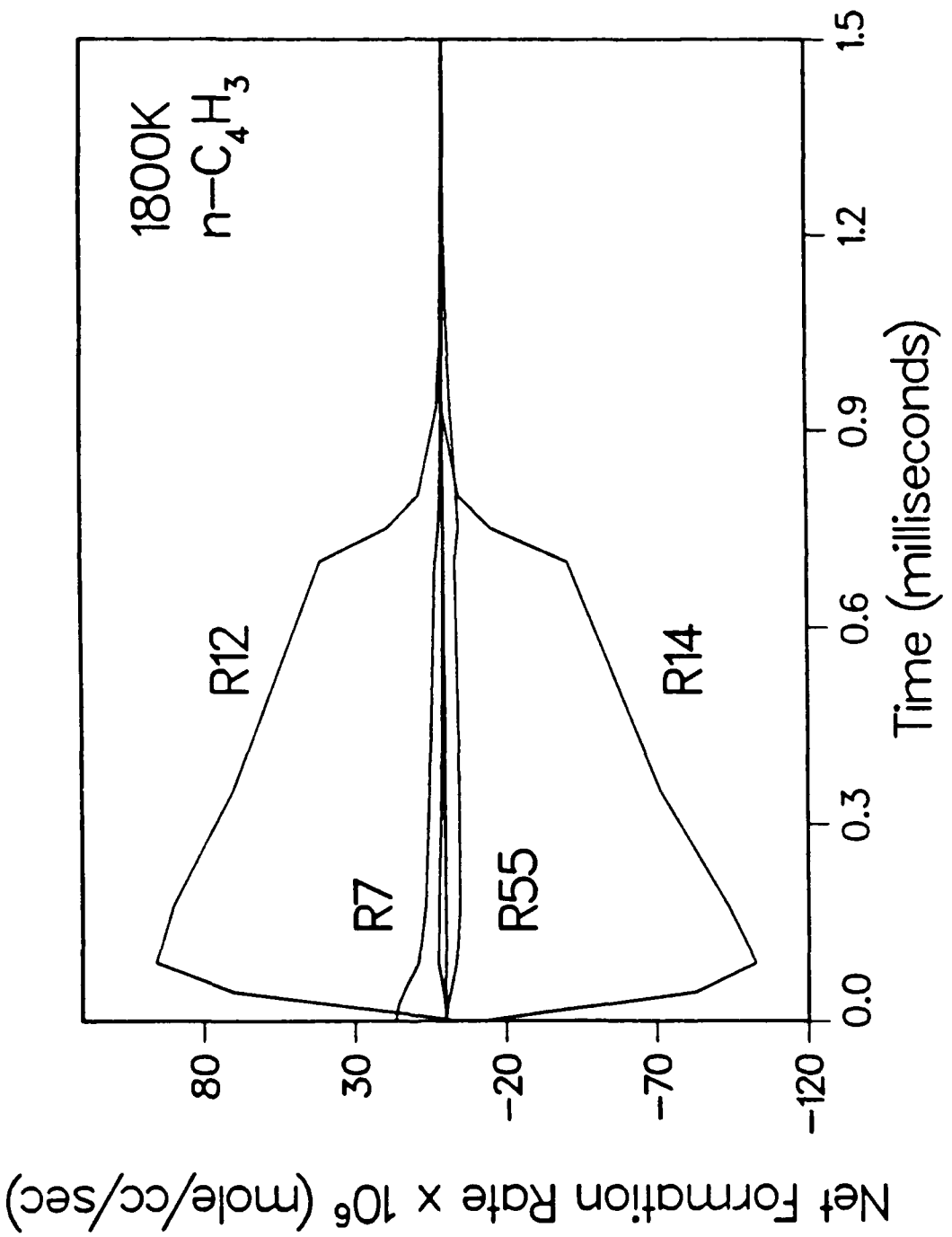
1800K
n–C4H3
R12
R7
R55
R14
80
30
–20
–70
–120
0.0
0.3
0.6
0.9
1.2
1.5
Time (milliseconds)
Net Formation Rate x 10⁶ (mole/cc/sec)

Fig. 3

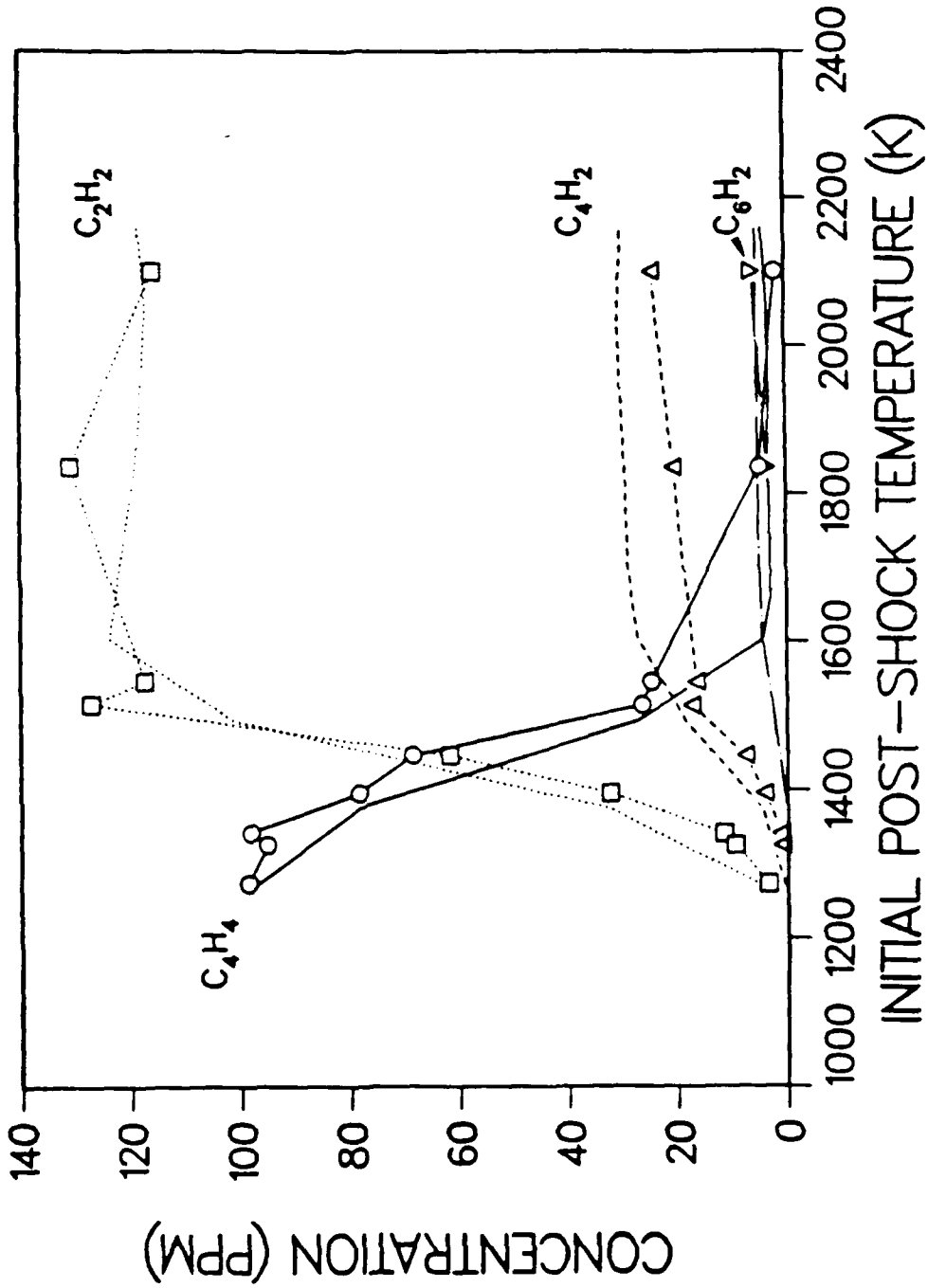
CONCENTRATION (PPM)
0
20
40
60
80
100
120
140
1000
1200
1400
1600
1800
2000
2200
2400
INITIAL POST-SHOCK TEMPERATURE (K)
C_2H_2
C_4H_2
C_6H_2
C_4H_4

Fig. 4

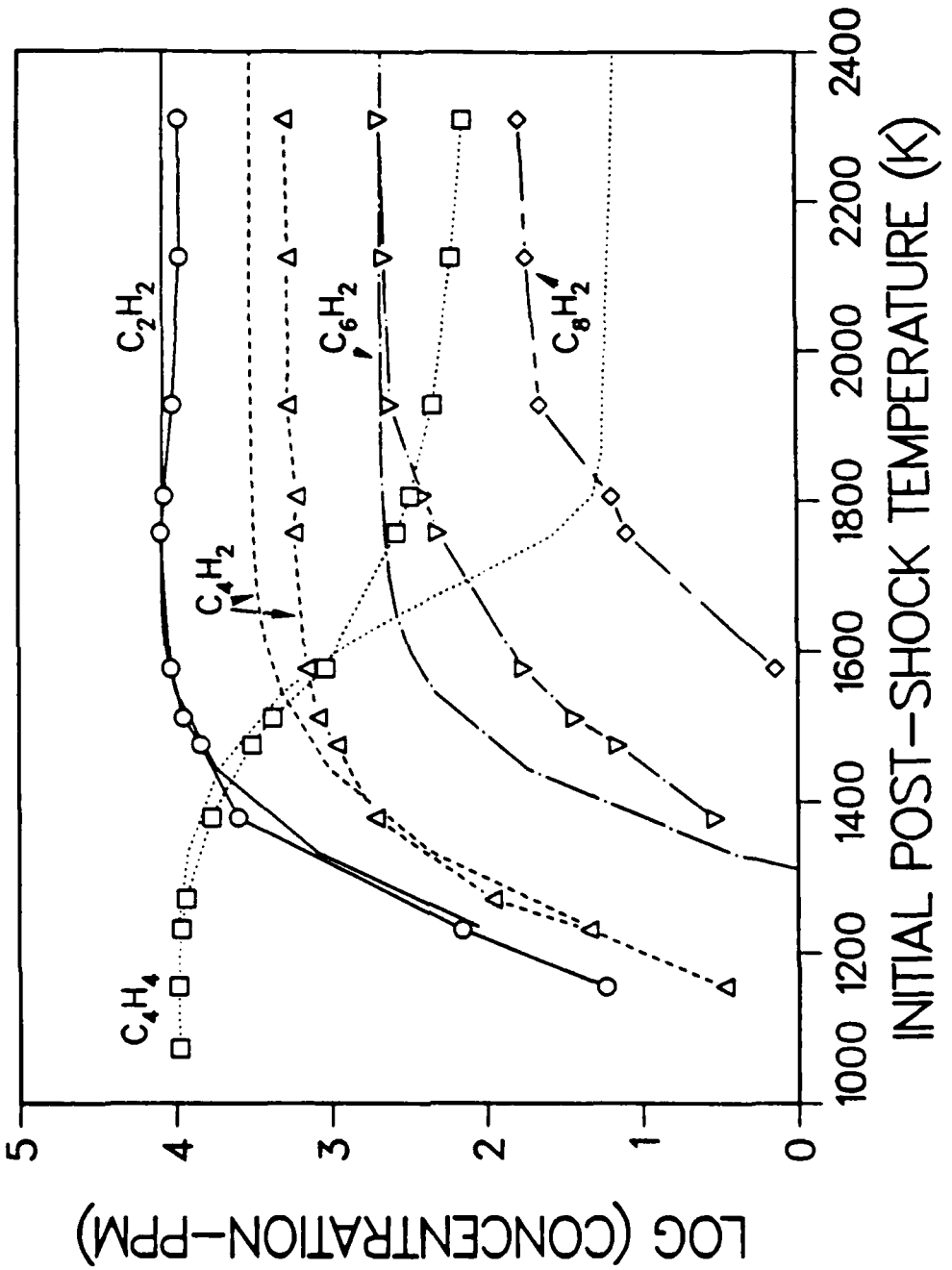
LOG (CONCENTRATION-PPM)
INITIAL POST-SHOCK TEMPERATURE (K)
0
1
2
3
4
5
1000
1200
1400
1600
1800
2000
2200
2400
C_2H_2
C_4H_2
C_6H_2
C_8H_2
C_4H_4

Fig. 5

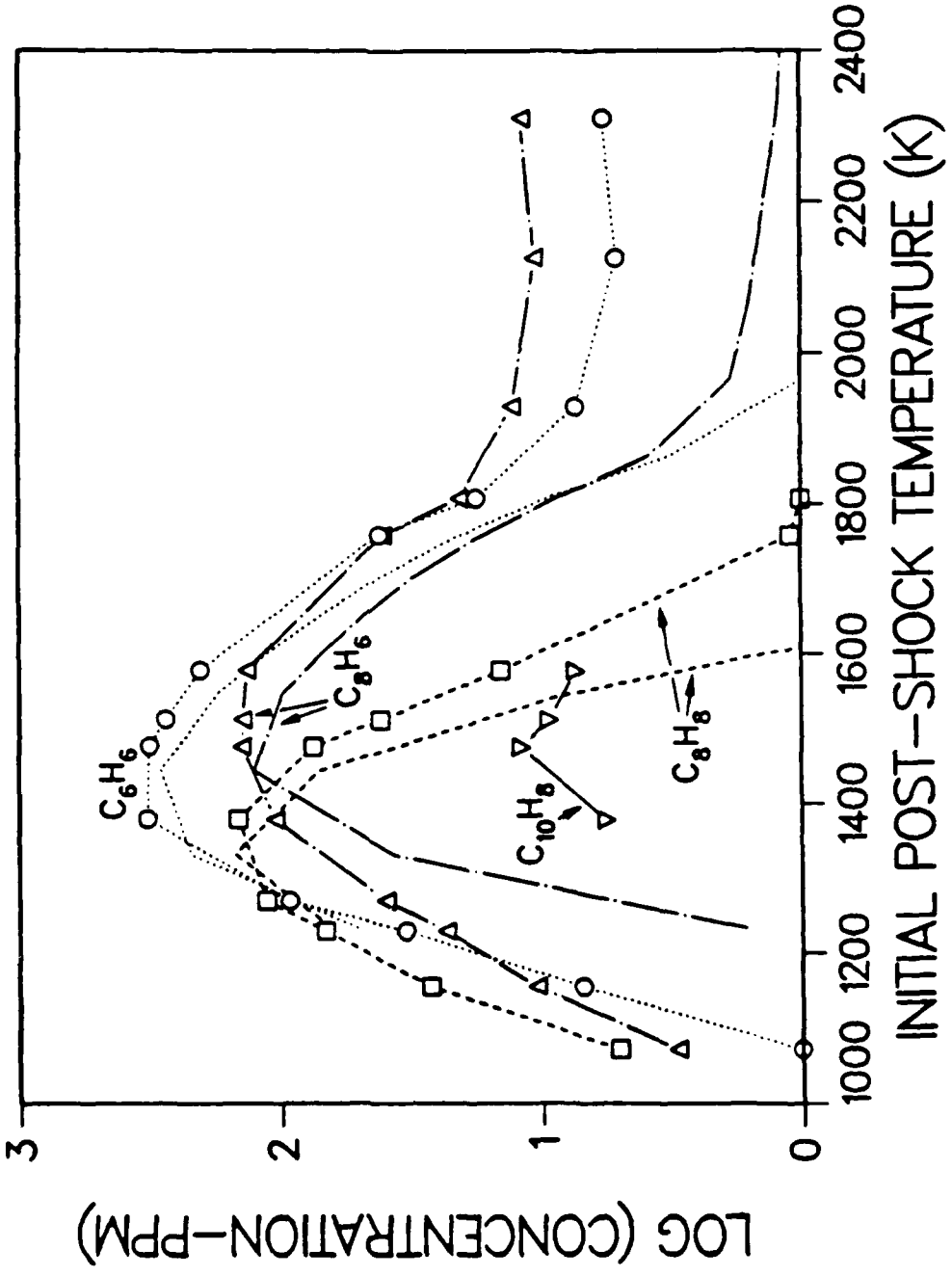
LOG (CONCENTRATION-PPM)
INITIAL POST-SHOCK TEMPERATURE (K)
0
1
2
3
1000
1200
1400
1600
1800
2000
2200
2400
C_6H_6
C_8H_6
$C_{10}H_8$
C_8H_8

APPENDIX II

Pyrolysis of Biacetyl in a Single-Pulse Shock Tube

by

M. B. Colket, III

United Technologies Research Center
East Hartford, Connecticut 06108

To Be Submitted to
Journal of Physical Chemistry

December 1986

Abstract

Biacetyl (2,3-butanedione) has been pyrolyzed in a single-pulse shock tube over the temperature range of 1050 to 2600°K, at total pressures near eight (8) atmospheres, dwell times of 600 microseconds and initial concentrations of 210 and 2040 ppm in argon. Final concentrations of pyrolysis products were determined by gas chromatography. Major products, initially, were ethane and carbon monoxide. Ethane production indicates the predominance of methyl radicals. Other products included methane, hydrogen, ethene, acetylene, diacetylene, propene, C_3H_4 (propyne + allene), benzene, styrene and phenylacetylene. Oxygenated products included acetone, ketene, and acetaldehyde. Detailed chemical kinetic calculations were made for comparison to the experimental profiles. The theoretical profiles were very similar to the experimental curves for most species. Principally, literature evaluations of rate constants were used for the calculations, although the rate for the initiation step,

$$(CH_3CO)_2 \rightarrow 2CH_3CO \quad (1),$$

$$\text{was } k_1 = 10^{16.3} \, e^{(-67000 \text{ cal/mole/RT})} \text{ sec}^{-1}$$

This value is about a factor of two above earlier, low temperature, determinations. Chemical mechanisms for the production of benzene and single ring aromatics which have been proposed in studies of acetylene pyrolysis significantly underpredict concentration of aromatics observed. It is possible that reactions involving methyl radicals that have not been included in the other mechanisms may contribute to ring formation. Methyl radical concentrations were calculated using a three-step and an 86-step mechanism. The three-step mechanism adequately describes methyl radical formation and destruction in the early phase of the pyrolysis.

Introduction

Addition of small concentrations of methane to combustion (1,2) has resulted in a significant augmentation in the production of soot. It is uncertain whether methane and/or methyl radicals effect soot production by accelerating processes related to pre-particle chemistry or by enhancing growth of existing soot particles. Benson (3) has proposed a chemical mechanism for production of aromatic rings from methyl radicals. This result suggests methyl accelerates pre-particle chemistry; however, Benson's model applies to an environment rich in methyl radicals and at temperatures which may be less than those during soot formation in practical combustion devices. The importance of the proposed mechanism during combustion in practical devices or during pyrolysis at elevated temperatures has not been established. Consequently, a series of experiments in which methyl radicals are added to the combustion or pyrolysis of fuels could be of interest. Biacetyl (2,3-butanedione) has been selected as a convenient source of methyl radicals since (1) it is not severly hazardous, (2) it produces a by-product (carbon monoxide) which can be traced easily but yet is relatively unreactive, and (3) thermal decomposition of its weak carbonyl-carbonyl bond (~68 kcal/mole) should produce acetyl, and then, methyl radicals. This work reports on results of pyrolyzing biacetyl in a single-pulse shock tube (SPST). The results are compared with detailed chemical kinetic calculations and the potential for the use of biacetyl as a source for methyl radicals during pyrolysis and combustion is discussed.

Description of Facilities

The SPST used in this program is 285 cm long and has a diameter of 3.8 cm (i.d.). The driver is 88 cm in length and can be tuned by shortening its length in 3.8 cm increments; the driven section is 197 cm long. An 11.7 liter "dump tank" is located in the driver (lower pressure) section 30 cm downstream of the diaphragm. Pressure profiles were determined using Kistler pressure transducers located 15.25 and 2.50 cm from the end wall. Arrival times were determined to within one microsecond using digitized pressure traces. Calculated quench rates are typically 10^5 K/sec or higher in the rarefaction wave. Starting pressures prior to filling are 0.2 μ and leak rates are less than 1μ/min. Post-shock temperatures were calculated based on the measured incident shock velocity and normal shock wave equations.

The procedures for performing an experiment are similar to those described in Tsang(4) except for an automated sampling system. The sample is collected at the endwall of the shock tube using 0.045 inch i.d. tubing heated to over 85°C. Approximately 30 milliseconds after the gas has been shock heated and cooled, a solenoid valve opens to the evacuated sample cell and then closes after 300 milliseconds. The sample storage vessel is all stainless steel with an internal volume of 25 cc.

The sampling volume is directly coupled to a low volume (<3 cc), heated inlet system of a Hewlett Packard 5880 A gas chromatograph. Typical injection

pressures are 0.5 atmospheres and are measured to within two percent using a calibrated pressure transducer. Three separate gas sampling valves are used to analyze the sample. The first injects samples onto a CP Sil 5 CB fused silica capillary column (from Chrompack, Inc.) followed by quantitative hydrocarbon analysis (up to C_{10} at ppm levels) via flame ionization. A second valve leads to a Molecular Sieve 5A, packed, stainless steel column and a single-filament, modulated thermal conductivity detector for analysis of hydrogen (to 5 ppm in a carrier of argon). (Helium (at 5 ppm), oxygen (at 0.1%) and nitrogen (at 0.1%) can also be detected in this system and provide verification of the integrity of the sample collection/analysis procedure.) The third valve is in series with a Carbosieve S-II column, a Ni catalyst for hydrogenation of carbon oxides(5), and a flame ionization detector. This system enables a duplication of the measurements of methane and C_2-hydrocarbons, as well as providing good sensitivity (~10 ppm) for the analyses of carbon monoxide and carbon dioxide. Based on repeated injections of calibrated samples, overall measurement accuracies are estimated to be approximately three to four percent. Calibration gases were stored in stainless steel cylinders with degreased valves and were heated to approximately 60°C prior to injection. Uncertainties in some gases for which samples were not readily available (e.g. C_4H_2, C_6H_2) are higher; however, since the FID response per non-oxygenated carbon atom is reasonably constant for low molecular weight hydrocarbons, estimated calibrations are probably accurate to within 20%. The uncertainty in the reported value of ketene was unknown due to its high reactivity. The reported values are believed to represent lower limits.

Argon (99.999% pure) was obtained from Matheson and was used as diluent. Biacetyl (97%, 2,3-butanedione) was obtained from Wiley Organics. Mixtures were made by partial pressure mixing. First, the liquid was degassed and then a portion vaporized into a large, evacuated stainless steel cylinder. Gas chromatographic analysis indicated total hydrocarbon impurities of final mixtures were less than 0.3% of the biacetyl concentration.

Experimental Results

Two series of runs at different initial biacetyl concentrations (2040 and 210 ppm in argon) have been completed. A single series represents several runs spanning a temperature range (e.g. 1100 to 1600°K). Dwell times (time prior to arrival of quenching wave) as measured from pressure traces were typically 600 $\pm$ 100 microseconds. Total pressures ranged from approximately seven to ten atmospheres. Final concentrations of reactant and products as a function of initial post-shock temperature are plotted in Figs. 1 and 2 for runs with initial concentration of 210 ppm biacetyl, and Figs. 3, 4 and 5 for runs with 2040 ppm biacetyl. The kinetics of the decomposition of biacetyl and initial product formation occurs below 1125°K for the duration of the SPST experiments. At higher temperatures, the decomposition is essentially complete. The two predominant products were ethane and CO. Detectable in lower concentrations (< 10% of major products) were methane, hydrogen, ethene, acetone, ketene, and acetaldehyde. The latter two existed in measurable

quantities only in the higher concentration experiments. Between 1150 and 1225°K the profiles for the above species flatten (except H_2 and C_2H_4). Above 1250, pyrolysis of ethane (and that of its pyrolysis products) becomes rapid so the remaining hydrocarbons convert principally to acetylenic species and hydrogen above 1800°K. Also of potential interest are low concentrations of propene, C_3H_4 (presumed to be principally methyl acetylene), benzene, phenylacetylene and styrene.

Modeling Results

Detailed chemical kinetic calculations have been performed using CHEMKIN(6), LSODE (7), and a version of a shock tube code originally developed by Mitchell and Kee (8), but modified to include quenching effects in an SPST(9). Quenching rates, based on experimental pressure traces and adiabatic expansion, were approximately 5×10^5 K/sec and varied depending on initial shock strength.

The chemical kinetic model describing biacetyl decomposition is based on a sequence of reaction steps from literature results(10-14) but modified slightly in accordance with the present experimental results. Reactions describing secondary pyrolysis of ethane and ketene were obtained principally from Warnatz's recent compilation(15). Estimates(16) for decomposition of acetone were made and rate measurements for the pyrolysis of acetaldehyde(17). In addition, a reaction sequence describing the pyrolysis of acetylene(9) is included. The complete chemical kinetic sequence is reproduced in Table I.

Comparison of the experimental profiles and the modeling results is shown in Figs. 1-5. The comparison is quite good for the major and many minor species. It will be noted that the experiment indicates the existence of a significant concentration of biacetyl at elevated temperatures, whereas the model shows virtually complete decomposition above 1200°K. The discrepancy is believed to be an experimental problem. During the sampling process, a portion of the gas collected is from the boundary layer near the walls of the shock tubes. These relatively cooler gases contain unpyrolyzed reactant. Previous results in this laboratory have shown that the reactant is always present in the sampled gases at concentrations approximately a few percent of the initial level.

The reaction sequence developed for low temperature results adequately describes the product distribution at high temperatures. The core reaction set includes

(1) $$CH_3COCOCH_3 \longrightarrow CH_3CO + CH_2CO$$

(2) $$CH_3CO \longrightarrow CH_3 + CO$$

(3a) $$CH_3 + CH_3COCOCH_3 \longrightarrow CH_4 + CH_2COCOCH_3$$

(3b) $$CH_2COCOCH_3 \longrightarrow CH_2CO + CH_3CO$$

(4) $CH_3+CH_3COCOCH_3 \longrightarrow CH_3CO+CH_3COCH_3$

(5) $CH_3+CH_3 \longrightarrow C_2H_6$

(5a) $CH_3+CH_2COCOCH_3 \longrightarrow C_2H_5COCOCH_3$

This sequence describes most of the observed products, i.e., C_2H_6, CO, CH_4, CH_3COCH_3, CH_2CO. 2,3-Pentadione is an important termination product (see Reaction 5a) at low temperatures, but, presumably due to the relative instability of the intermediate ($CH_2COCOCH_3$) at higher temperatures, 2,3-pentadione was observed only in trace concentrations during the present experiments.

At low temperatures, the principal products are carbon monoxide, methane, acetone, and 2,3-pentadione with small concentrations of ethane and ethene. The present results differ substantially in that the major species near 1100°K are ethane and carbon monoxide. The predominance of these species is explained by the sequence, Reactions 1, 2, followed by 5. This result is not surprising considering the tabulation(10) of product ratios (C_2H_6/CO and CH_4/C_2H_6) as a function of temperature. Sherzer and Plarre's compilation(10) is indicative of the decreasing chain length (rate of chain propagation/rate of initiation) with increasing temperature. At 648°K, data from Knoll, et al(11) suggests that the chain length is approximately 6, whereas data from Sherzer and Plarre at 905°K indicate a chain length slightly over unity. The present work indicates a chain length of approximately 0.1 at 1050 to 1100°K. (For the above calculations, chain length is assumed to be

$$([CH_4] + [CH_3COCH_3])/([C_2H_6] + [C_2H_5COCOH_3])).$$

Calculations suggest the concept of chain length becomes slightly awkward at higher temperatures since much of the initial biacetyl is decomposed before subsequent abstraction or recombination reactions become significant. For example, calculations indicate that at conditions of 200 ppm biacetyl at 1300°K (8 atmospheres), 50% of the biactyl decomposes before methyl radicals attain "quasi steady-state" concentrations (elapsed time is approximately 7 microseconds). Estimates of the chain length under these quasi-steady conditions are less than 0.01. Consequently, greater than 99% of the decomposed biacetyl converts to methyl radicals or products (principally ethane) of methyl radical recombination. These results verify the original expectation that biacetyl is a good source of methyl radicals at elevated temperatures.

Initiation Reaction

Published rate coefficients for the initial thermal decomposition have been reviewed by Sherzer and Plarre (10). Activation energies are consistent

with the strength of the carbonyl-carbonyl bond (D(ROC-COR) = 67.8 kcal/mole). In this work, highly accurate rate determinations were not made, since the principal objective of this work was to verify that biacetyl could be a high temperature source of methyl radicals. (In order to determine rates accurately, the experiments would have been extended to a lower temperature and relative rate measurements (4) would have been performed). Nevertheless, the model results were noticeably affected by selected rate constants and some adjustments to extrapolated expressions developed from low temperatures were indicated. The rate constant expression for initiation, $k_1 = 10^{16.3}$ exp (-67000 cal/mole/RT) sec^{-1}, was selected so as to provide reasonable agreement with the present results as well as to be consistent with the earlier work. The uncertainty in this expression is about a factor of two or three. Comparison of the above expression and previous results is shown in the Arrhenias plot in Fig. 6. The rate used in this work is about a factor of two higher than relatively recent results.

Carbon Monoxide and Ethane Formation

Carbon monoxide is a direct result of Reactions 1 and 2. The other major product, ethane, is formed from the recombination of methyl radicals (R5). Methyl radicals may also produce ethyl radicals and H-atoms (R6), or ethylene and hydrogen (R7). In addition, Olsen and Gardiner(18) have suggested the reaction

(R8) $$CH_4 + CH_2 \longrightarrow CH_3 + CH_3$$

the reverse of which can be of interest under conditions of high methyl radical concentration. All of these methyl-methyl reactions have been included in the model, although the Olsen and Gardiner rate constant for R-8 has been decreased by approximately a factor of 100 (see later discussion regarding methylene reactions). The relative value of the rate constants at 1050K ($k_5/k_6 = 6210$, $k_5/k_7 = 6930$, and $k_5/k_8 = 14300$) ensures the dominance of Reaction 5, and therefore ethane formation. For k_5, k_6 and k_7, recommended rate expressions(15) were used.

As temperature increases above 1250°K, ethane formed by Reaction 5 decomposes due to H-atom abstraction via radical attack and the profiles (see Figs. 1 and 3) for ethane decrease substantially. The model at elevated temperatures appears to underpredict slightly the amount of ethane decomposition; presumably this is due to inaccuracies in predicting H-atom concentrations.

Methane Formation

Methane is formed principally via Reaction 3a over the low temperture portion of the present experiments (approximately 1050 - 1225K). k_{3a} was determined by performing a 3-parameter, least-squares-fit on earlier measurements. Previous work for Reaction 3a covered the temperature range 350 to 905K and indicates a slight increase in activation energy with increasing

temperature (see Table 6 from Ref. 10). The expression used in this work is

$$k_3 = 512T^{2.87} \exp(-6430 \text{ cal/mole/RT}) \text{ cc/mole/sec}$$

and is compared to previous determinations in Fig. 7. The slight curvature in this Arrehenius plot and the substantial temperature exponent are consistent with rate measurements and calculations for other H-atom abstraction reactions by methyl radicals(22). As can be seen in Figs. 1 and 3, the above expression provides a reasonable estimate of methane production for the low temperature regime. For the modeling work, it was assumed that Reaction 3 was the overall process (combination of 3a and 3b)

$$CH_3 + CH_3COCOCH_3 \longrightarrow CH_4 + CH_2CO + CH_3CO$$

which is allowed to proceed only in the forward direction. This assumption is reasonable, considering the half-life of the $CH_2COCOCH_3$ radical ($t_{1/2} = .693/k_{3b} = 7.5$ and 0.013 microseconds at 1100K and 1500K, respectively). The rate expression for k_{3b} is taken from Ref. 10, i.e., $k_{3b} = 10^{15.3} \exp(-52000/RT) \text{ sec}^{-1}$). An estimate of its maximum concentration can be obtained from the steady-state expression:

$$\frac{[CH_2COCOCH_3]}{[CH_3]} = k_{3a}\frac{[CH_3COCOCH_3]}{k_{3b}}$$

Assuming the initial concentration of biacetyl to be 0.2% in 8 atmospheres of argon, the ratio $[CH_2COCOCH_3]/CH_3$, is calculated to be about 4×10^{-3}, and 3×10^{-5} at 1100 and 1500K, respectively. Thus, the $CH_2COCOCH_3$ radical appears to play a relatively minor role (other than in Reactions 3a and 3b), and use of an overall step (Reaction 3) at temperatures of this study, appears justified. As temperature is increased, biacetyl decomposes within the first few microseconds (via Reaction 1) and is not available for H-atom abstraction to produce methane via Reaction 3. Methyl radicals produced in the decomposition virtually have no collision partners other than argon, carbon monoxide, themselves (to produce principally ethane via recombination), or ethane. Consequently, above 1225K, a principal mechanism for formation of methane is

(9) $$CH_3 + C_2H_6 \longrightarrow CH_4 + C_2H_5$$

(10) while the recombination process $CH_3 + H \longrightarrow CH_4$

makes a substantial contribution. At yet higher temperatures, the reactions $CH_3 + C_2H_4 \rightarrow CH_4 + C_2H_3$, $CH_3 + H_2 \rightarrow CH_4 + H$ play a significant role.

Formation of Hydrocarbon Oxygenates

Ketene, as previously described(10-12), is formed in Reactions 3(a and b). Reaction 3 has been discussed in the previous section. Assuming ketene is

relatively unreactive, its concentration at low temperatures should be nearly equivalent to that of methane. As indicated by both the modeling and experimental results, the high reactivity substantially depresses its concentration. The concentration of ketene is limited by its decomposition, such as through

(11) $$CH_3 + CH_2CO \rightarrow C_2H_5 + CO$$

followed by

(12) $$C_2H_5 \rightarrow H + C_2H_4$$

and, possibly,

(13) $$H + CH_2CO \rightarrow CH_3 + CO$$

Unimolecular decomposition of ketene via

(14) $$CH_2CO \rightarrow CH_2 + CO$$

is negligible at low temperatures, but at higher temperatures, the model indicates that the reverse of this reaction contributes to ketene formation. Under these conditions, methylene arises from methyl radical disproportionation (Reaction 8). Although ketene is not detected in the lower concentration experiments, the model predicts ketene concentrations similar to those of acetone in Figure 1. The discrepancy between the experiment and the model may be due to uncertainties in the kinetics and mechanisms of ketene decomposition, as well as probable errors associated with collecting and analyzing ketene at parts-per-million concentrations.

In addition, substantial uncertainty in the calculated ketene profiles is related to the methylene radical. In this work, no attempt has been made to identify the separate roles of the ground-state triplet or the low-lying singlet state. In a review of the kinetics of the methylene radical, Laufer (18) identifies the ground-state triplet as being relatively unreactive at room temperatures, whereas reactions involving the singlet are rather fast. If the principal species in this system is the triplet, then several of the rate constants listed in Table I (involving CH_2) are orders of magnitude too high. Intersystem crossing, however, appears to be quite fast. Using rate constants from Laufer's review(23), the half-life of the $^1A_1 \rightarrow {}^3B_1$ collisional deactivation is on the order of tens of nanoseconds in eight atmospheres of argon. Assuming that collisional activation is also fast and since the singlet is only 7 to 12 kcal/mole above the ground state(24), then the singlet may exist at elevated temperatures according to a Boltzmann distribution. Consequently, H-atom abstraction reactions from hydrocarbons by singlet methylene may play significant roles. In this work, k_8 and k_{34} were assumed to be 5×10^{12} exp(-10000 cal/mole/RT) cc/mole/sec to account for the competitive effects of the reactivity of $^1CH_2$ and the dual nature of CH_2. Using these rates, R_8 and R_{34} played a minor role in the

concentration profiles of methylene.

The source of acetone has been identified(13) to be the concerted step, Reaction 4. This also represents an overall process which, as previously reported, can be written

(4) $CH_3 + CH_3COCOCH_3 \rightleftharpoons CH_3CO(CH_3)COCH_3 \rightleftharpoons CH_3COCH_3 + CH_3CO$

The rate constant used in this work is that determined by Scherzer and Plarre(10) over the temperature regime 822-905K, i.e.

$$k_4 = 1.58 \times 10^{11} \exp(-8600 \text{ cal/mole/RT}) \text{ cc/mole/sec}$$

This rate agrees with extrapolations of previous determinations at yet lower temperatures (11-13). As seen in Fig. 1, this expression appears to underpredict the production of acetone at low concentrations of biacetyl. A rate three to four times higher at 1050K would be required to match the experimental profile. Such a shift appears unwarrented in view of the previous work; besides, it would lead to an overprediction of acetone at higher biacetyl concentrations. It is possible that significant concentrations of acetone can be produced in the lower-temperature boundary layer of the SPST. At 500-600K, for example, the rate constants k_3 and k_4 are nearly identical, the chain length grows, and acetone becomes a dominant product species.

The radical recombination process, R15, has been included in the model although it contributes negligibly to acetone production. Above 1100K, acetone decomposes principally via Reaction 16, i.e.

(16a) $$CH_3 + CH_3COCH_3 \rightarrow CH_4 + CH_2COCH_3$$

(16b) $$CH_2COCH_3 \rightarrow CH_2CO + CH_3$$

although only the overall reaction was included in the model calculations. The rate constant was equated to that for Reaction 3.

Acetaldehyde was not reported as a product in the low temperature studies. In this work, the principal mechanism for acetaldehyde formation is believed to be

(17) $CH_3COCOCH_3 + H \rightleftharpoons CH_3CO(H)COCH_3 \rightleftharpoons CH_3CHO + CH_3CO$

This process is analagous to that for acetone formation and the reverse of the process suggested(25) for acetone formation during pyrolysis of acetaldehyde. The rate constant assigned to the overall reaction is

$$CH_3COCOCH_3 + H \rightarrow CH_3CHO + CH_3CO$$

$$k_{17} = 10^{13} e^{-5000/RT} \text{ cc/moles/sec.}$$

H-atoms participating in Reaction 17, are produced principally during ethyl radical decomposition

(12) $C_2H_5 \rightarrow C_2H_4 + H$

which follows either ethane (R9) or ketene (R11) decomposition.

The rate constant (k_{17}) used in this work depends both on mechanisms for the production of H-atoms (Reaction 6 and 12) and competitive steps for the loss of H-atoms, for example

(18) $H + (CH_3CO)_2 \rightarrow CH_2COCOCH_3 + H_2$

Due to the importance of step 11 to the production of ethyl radicals and, therefore, H-atoms at low temperature, the production of acetaldehyde is strongly dependent on the concentration of ketene. Consequently, the rate constant, k_{17}, recommended in this work may be in error by as much as a factor of 10. Reactions 19 and 20 (followed by 21) were included to account for decomposition of acetaldehyde.

Formation of C_2H_4 and H_2

Figures 2 and 4 show that ethylene production matches hydrogen production from 1050 to 1400K. Conceptually, this result is due to the overall process

(7) $(CH_3CO)_2 \rightarrow C_2H_4 + H_2 + CO$

although, as previously discussed, most of the biacetyl produces ethane and carbon monoxide at low temperatures. At the lowest temperatures of this work, modeling indicates that most of ethylene and hydrogen are produced via a sequence involving ketene, i.e.

(3a) $CH_3 + (CH_3CO)_2 \rightarrow CH_4 + CH_2COCOCH_3$

(3b) $CH_2COCOCH_3 \rightarrow CH_2CO + CH_3CO$

(11) $CH_3 + CH_2CO \rightarrow C_2H_5 + CO$

(12) $C_2H_5 \rightarrow C_2H_4 + H$

(18a) $H + (CH_3CO)_2 \rightarrow H_2 + CH_2COCOCH_3$

(22) $H + C_2H_6 \rightarrow H_2 + C_2H_5$

although a portion of the H-atoms are lost to Reactions 10 and 17.

At slightly higher temperatures (~1175K), the lifetime of biacetyl becomes very short, so it can no longer initiate the above ethene formation route via

Reaction 3a. Ketene is still formed, according to the model calculations, by recombination of methylene and CO (R-14), so some ethene is formed via the R11, R12 reaction sequence. In addition, a small portion of ethene arises from

$$CH_3 + CH_3 \rightarrow C_2H_4 + H_2$$

although ethane is the preferred recombination product. As temperature is increased further, Reactions 9 or 19 (H-atom elimination from ethane) followed by R12 (ethyl decomposition) become the most significant steps for H-atom formation. H-atoms, under these conditions, will react with ethane, since the parent, biacetyl, has been virtually eliminated within a few microseconds through thermal decomposition.

Above 1400°K, ethylene concentrations fall off as hydrogen continues to increase. This behavior is a result of thermal decomposition of ethylene to acetylene and hydrogen (overall process).

Formation of Other Aliphatic Species

Reactions 20 and 21 have been included to account for the presence of propene and propyne (possibly some allene) in the pyrolysis products.

(23a) $$CH_3 + C_2H_4 \rightarrow C_3H_7$$

(23b) $$C_3H_7 \rightarrow C_3H_6 + H$$

(24a) $$CH_3 + C_2H_2 \rightarrow C_3H_5$$

(24b) $$C_3H_5 \rightarrow C_3H_4 + H$$

Overall rate constants for Reactions 23 and 24 were assigned the values determined(26) for Reactions 23a and 24a respectively. Figs. 2-4 show a comparison between the model and the experimental results. The model appears to underestimate the production of propene at low temperatures, although the total C_3-hydrocarbon prediction is in good agreement with the experiment at slightly higher temperatures. The difference between the model and experiment at low temperatures is uncertain.

Acetylene is formed by decomposition of ethylene, i.e.

$$R + C_2H_4 \rightarrow RH + C_2H_3$$

and

$$C_2H_3 \rightarrow C_2H_2 + H$$

Further pyrolysis of acetylene to form diacetylene is described by a kinetic sequence presented recently(9) for the pyrolysis of acetylene.

Vinylacetylene is produced from a variety of steps, including:

(-81) $C_2H + C_2H_3 \rightarrow C_4H_4$

(-43) $H + i\text{-}C_4H_3 \rightarrow C_4H_4$

(54) and $C_2H_3 + C_2H_2 \rightarrow n\text{-}C_4H_5$

(76) followed by $n\text{-}C_4H_5 \rightarrow C_4H_4 + H$

where the radicals C_2H, C_2H_3 and $i\text{-}C_4H_3$ (CH_2:CC:CH) are produced during pyrolysis of acetylene. The relative contributions depend on temperature and reaction time. This conclusion (regarding the source of vinylacetylene) differs significantly from that obtained during an analysis of acetylene pyrolysis near 1200°K. In the latter case, it was found(9) that Reaction 54 followed by 76 dominated. The comparison between the experiment and model are reasonable considering the concentration level of vinylacetylene (see Fig. 5).

Formation of Aromatics

Production of aromatics is typically underpredicted by more than an order of magnitude using the chemical kinetic model in Table I. For the conditions of Fig. 5, predictions of any single aromatic are less than 100 parts per billion. The model includes reactions such as

(77) $C_2H_2 + n\text{-}C_4H_5 \rightarrow 1\text{-}C_6H_7 \rightarrow C_6H_6 + H$

(75) $C_2H_3 + C_4H_4 \rightarrow 1\text{-}C_6H_7 \rightarrow C_6H_6 + H$

(-85),(-86) and $C_2H_2 + n\text{-}C_4H_3 \rightarrow 1\text{-}C_6H_5 \rightarrow$ phenyl

which have been suggested(9) to be important for the production of aromatic rings during pyrolysis of acetylene and vinylacetylene. ($1\text{-}C_6H_7$ and $1\text{-}C_6H_5$ are linear compounds). The inability of these steps to describe the production of aromatics during biacetyl pyrolysis suggests that (1) concentrations of hydrocarbon radicals, specifically $n\text{-}C_4H_5$, $n\text{-}C_4H_3$ and C_2H_3, are significantly underestimated using the present model; (2) rate constants for one or more of the above reactions are too low; or (3) other mechanisms for the formation of aromatic rings contribute significantly. Uncertainty due to (1) is certainly plausible due to the complexity of the entire mechanism. The mechanism is supported, however, due to the recent success in modeling aromatic formation(9) and to consistency with a review of rate constants(15). Nevertheless, few or no determinations of absolute rate constants for many of the reactions exist. The problem is exacerbated by the uncertainty in the thermodynamics of vinylic-type radicals(27) which reduces the accuracy of thermochemical estimation techniques(16). Uncertainty due to (2) is probably not as significant since absolute rate constants for Reactions 77 and -85 are consistent with or already higher than other determinations.

Underestimation of aromatics due to (3) seems quite probable, especially in light of the recent suggestion(3) that low molecular weight aliphatics grow through sequential addition of methyl radicals and then cyclize to form benzene. Unfortunately, due to the relatively low concentrations of aromatics and probable intermediates, this mechanism could not be confirmed for the present reaction system.

Discussion

Pyrolysis of biacetyl above 1000°K demonstrates the principal process to be

(1) $$CH_3COCOCH_3 \rightarrow 2CH_3CO$$

(2) $$CH_3CO \rightarrow CH_3 + CO$$

(5) $$CH_3 + CH_3 \rightarrow C_2H_6$$

while subsequent decomposition of ethane and other secondary processes account for the remainder of the products. To demonstrate the applicability of this simplified mechanism in a concrete fashion, calculations for time-dependent methyl radical concentrations were performed using this simple three-step mechanism and the full 86-step mechanism presented in Table I. For initial concentrations of 2040 ppm biacetyl, methyl profiles are compared in the log-log plot in Fig. 8 for a range of initial temperatures. As apparent from this figure, the drastically reduced sequence provides a wholly satisfactory procedure for estimating the methyl radical profiles.

Considering the high conversion efficiency of biacetyl to methyl, biacetyl does appear to be a good source of methyl radicals under shock tube conditions. One concern, however, is that the methyl radical production rate can be so high initially that methyl recombination may become very fast. In order for reactions involving methyl radical addition to compete with recombination

(x) $$CH_3 + R'H \rightarrow \text{adduct}$$

(5) $$CH_3 + CH_3 \rightarrow C_2H_6$$

then the expression $k_x[R'H] \sim k_5[CH_3]$ should be valid. Here, R'H represents an olefinic or acetylenic molecule. Since $k_5 \sim 10^{13}$ and k_x for addition reactions are on the order of 5×10^{10} (depending on the temperature and reaction in question); then [R'H] should be approximately 200 times greater than the methyl radical concentration. Biacetyl rapidly converts on a two to one basis to methyl radicals and therefore initial reactant to initial biacetyl concentrations ought to be on the order of 400. This ratio is obviously flexible depending on the temperature and reactants in question. At 1100°K, for example, peak CH_3 concentrations are about 50 times smaller than that at 1500°K. In addition, other practical

considerations such as the ability to measure accurately product distributions may encourage reactant/biacetyl ratios to be in the range of 10 to 100.

In conclusion, thermal decomposition of biacetyl appears to be a very rapid source of methyl radicals at high temperatures. Unfortunately, the high rate of methyl radical production results in rapid ethane formation. Under many conditions, this may be satisfactory; for others, a slower mechanism for release of methyl radicals may be required. Addition of methane may prove to be a useful alternative under such conditions.

Modeling the decomposition of biacetyl in the range of 1050 to 1100^{o}K is in excellent agreement with experimental results for a wide variety of products. The modeling work supports the mechanisms and rate constants determined previously for biacetyl pyrolysis at lower temperatures as well as mechanisms of pyrolysis for methane and C_2-hydrocarbons.

References

1. Haynes, B. S., Jander, H., Matzing, H., and Wagner, H. Gg.: Nineteenth Symposium (International) on Combustion, The Combustion Institute, p. 1379-1385, Pittsburgh, 1982.

2. Zabielski, M.F.: Personal communication, 1986.

3. Benson, S.W.: Personal communication, 1986.

4. Tsang, W.: Shock Waves in Chemistry, (Ed. by A. Lifshitz, Marcel Dekker, Inc., New York,) p. 59-129, 1981.

5. Colket, M.B., Naegeli, D.W., Dryer, F.L., and Glassman, I., Env. Sci. Tech. 8, 43 (1974).

6. Kee, R.J., Miller, J.A., Jefferson, T.H.: "CHEMKIN: A General-Purpose, Problem-Independent, Transportable, Fortran Chemical Kinetics Code Package", Sandia Laboratories, SAND80-8003, March, 1980.

7. Hindmarsh, A.C.: "LSODE and LSODI, Two New Initial Value Differential Equation Solvers", ACM SIGNUM Newsletter, 15, No. 4, December 1980.

8. Mitchell, R.E., and Kee, R.J.: "A General-Purpose Computer Code for Predicting Chemical Kinetic Behavior behind Incident and Reflected Shocks", Sandia National Laboratories, SAND82-8205, March 1982.

9. Colket, M.B., "The Pyrolysis of Acetylene and Vinylacetylene in a Single-Pulse Shock Tube", to be presented at the Twenty-first Symposium (International) on Combustion, Munich, Germany, Aug. 3-8, 1986.

10. Scherzer, K., and Plarre, D.: Z. Phys. Chemie, 256, 660-672 (1975).

11. Knoll, H., Scherzer, K., and Geiseler, G.: I.J.C.K. 5, 271-284 (1973).

12. Hole, K.J., and Mulcahy, M.F.R., J. Phys. Chem., 73, 177-185 (1969).

13. Knoll, H., Schliebs, R., and Scherzer, K., Reaction Kinetics and Catalysis Letters, 8, 469-475 (1978).

14. Schliebs, R., Knoll, H. and Scherzer, K., I.J.C.K. 9, 349-359 (1977).

15. Warnatz, J.: "Rate Coefficients in the C/H/O System", Chapter 5 in Combustion Chemistry, Ed. W. C. Grdiner, Jr., Springer Verlag, New York, 1984.

16. Benson, S.W.: Thermochemical Kinetics, J. Wiley and Sons, New York (1976).

17. Colket, M.B., Naegeli, D.W., and Glassman, I.: I.J.C.K. 7, 223 (1975).

18. Olsen, D.B., and Gardiner, W.C., Combust. Flame 32, 151-161 (1978).

19. Rice, F.O., and Walters, W.D., J. Chem. Phys. 7, 1015 (1939).

20. Guenther, W.B., Whiteman, C.A., and Walters, W.D., J. Am. Chem. Soc. 77, 2191 (1955).

21. Ausloos, P., and Steacie, E.W.R., Canad. J. Chem. 33, 39 (1955).

22. Furue, H., and Pacey, P.D.: J. Phys. Chem. 90, 397 (1968).

23. Laufer, A.H.: Reviews of Chemical Intermediates 4, 225-257 (1981).

24. Nichols, J.A. and Yeager, D.L.: Chem. Phys. Letters 84, 77-85 (1981).

25. Batt, L.: J. Chem. Phys. 47, 3674 (1967).

26. Holt, P.M., and Kerr, J.A.: I.J.C.K. 9, 185-200 (1977).

27. Sharma, R.B., Semo, N.M., and Koski, W.S.: I.J.C.K. 17, 831-833 (1985).

28. Kiefer, J.H., Kapsalis, S.A., Al-Alami, M.Z., and Budach, K.A.: Combust. Flame 57, 79 (1983).

29. Tanzawa, T., and Gardiner, W.C., Jr.: Combust. Flame 39, 241 (1980), also J.Phys.Chem. 84, 236 (1980).

30. Miller, J.A., Mitchell, R.E., Smooke, M.D., and Kee, R.J.: Nineteenth Symposium (International) on Combustion, p. 181, The Combustion Institute, 1982.

31. Kiefer, J.H., Mizerka, L.J., Patel, M.R., and Wei, H.-C., J.Phys.Chem. 89, 2013 (1985).

32. Colket, M.B.: "Pyrolysis of C_6H_6", presented at American Chmeical Society, New York City National Meeting, Division of Fuel Chemistry, preprints, April 13-16, 1986.

33. Fujii, N., and Asaba, T.: Fourteenth Symposium (International) on Combustion, p. 433, The Combustion Institute, Pittsburgh, 1973.

34. Mallard, W.G., Fahr, A., and Stein, S.E.: "Rate Constants for Phenyl Reactions with Ethylene and Acetylene", Paper No. 92, Chem.Phys.Proc. Comb., ES/CI, Dec. 3-5, Clearwater Beach, Fla., 1984.

35. Weissman, M. and Benson, S.W.: Int'l.J.Chem.Kin. 16, 307 (1984).

TABLE I
SET OF REACTIONS AND RATE COEFFICIENTS
$\log k = \log A + n \log T - E/(2.303RT)$ *

	Reactions	Forward rate constant			Reverse rate constant			
		A	n	E	A	n	E	Ref
1	BA=2CH3CO	16.30	0.00	67.0	12.09	0.87	2.2	PW *
2	CH3CO=CH3+CO	12.48	0.00	16.7	0.89	2.76	-2.3	15
3	CH3+BA-CH4+CH2CO+CH3CO	2.71	2.87	6.4	0.00	0.00	0.0	PW
4	CH3+BA=CH3CO+AT	11.20	0.00	8.6	14.87	-0.56	24.9	10
5	2CH3=C2H6	14.38	-0.40	0.0	25.45	-2.57	93.5	15
6	2CH3=C2H5+H	14.90	0.00	26.5	22.15	-1.47	19.9	15
7	2CH3=C2H4+H2	16.00	0.00	32.0	20.37	-0.72	90.1	15
8	CH4+CH2=2CH3	12.70	0.00	10.0	11.47	0.14	13.8	PW
9	C2H6+CH3=C2H5+CH4	-0.26	4.00	8.3	0.20	4.09	15.0	15
10	CH4=CH3+H	14.70	0.00	100.4	10.42	0.61	-6.5	15,PW
11	CH2CO+CH3=C2H5+CO	12.85	0.00	3.0	14.11	-0.06	26.9	PW
12	C2H5=C2H4+H	13.30	0.00	39.7	10.34	0.61	0.4	15
13	CH2CO+H=CH3+CO	12.85	0.00	3.0	6.86	1.41	33.5	PW
14	CH2CO=CH2+CO	14.00	0.00	71.0	4.97	1.89	-9.1	15,PW
15	CH3CO+CH3=AT	12.00	0.00	0.0	19.88	-1.43	81.2	PW
16	CH3+AT-CH4+CH2CO+CH3	11.20	0.00	8.6	0.00	0.00	0.0	10,PW
17	H+BA=CH3CHO+CH3CO	13.00	0.00	5.0	8.05	1.34	24.2	PW
18	H+BA-H2+CH2CO+CH3CO	13.30	0.00	5.0	0.00	0.00	0.0	PW
19	CH3+CH3CHO=CH4+CH3CO	-7.40	6.10	1.7	-2.38	5.02	24.5	17,15
20	CH3CHO=CH3+HCO	15.85	0.00	81.7	6.81	1.74	-5.1	17
21	HCO+M=CO+H+M	14.40	0.00	16.8	12.59	0.55	0.7	15
22	C2H6+H=C2H5+H2	2.73	3.50	5.2	-1.01	4.35	9.1	15
23	CH3+C2H4=C3H6+H	11.30	0.00	7.3	17.68	-1.51	-0.6	26
24	CH3+C2H2=C3H4+H	11.79	0.00	7.7	17.02	-1.10	1.5	26
25	CH3+C2H5=C3H8	12.85	0.00	0.0	22.57	-2.02	88.1	15
26	C2H5+H=C2H4+H2	12.27	0.00	0.0	9.39	0.76	64.7	18
27	C2H4+CH3=C2H3+CH4	11.62	0.00	11.1	10.86	0.26	10.7	15
28	CH4+C2H=CH3+C2H2	12.70	0.00	0.0	13.25	-0.36	20.8	PW
29	CH4+H=CH3+H2	4.34	3.00	8.8	0.15	3.75	5.9	15
30	CH3+M=CH2+H+M	16.67	0.00	93.2	13.62	0.47	-17.4	18
31	CH3+H=CH2+H2	14.26	0.00	15.1	11.29	0.62	8.5	18,PW
32	CH3+CH2=C2H4+H	13.62	0.00	0.0	20.96	-1.34	64.6	18,PW

* NOTES: Units for A: cc,moles,sec.
Units for E: kcal/mole.
"=" indicates forward and reverse rates included in the model
"-" indicates forward rate only included in model
PW indicates rate evaluated from the present work
BA = biacetyl (CH3COCOCH3)
AT = acetone (CH3COCH3)
Reverse rates calculated from forward rates and thermchemistry

TABLE I (continued)
SET OF REACTIONS AND RATE COEFFICIENTS
logk = logA + nlogT - E/(2.303RT) *

	Reactions	Forward rate constant			Reverse rate constant			
		A	n	E	A	n	E	Ref
33	2CH2=C2H2+H2	13.50	0.00	0.0	18.71	-0.81	130.7	18
34	CH2+C2H6=CH3+C2H5	12.70	0.00	10.0	11.93	0.23	20.5	PW
35	C2H4+M=C2H3+H+M	16.16	0.00	81.8	11.12	0.87	-25.5	28
36	C2H4+H=C2H3+H2	14.84	0.00	14.5	9.88	1.02	11.2	29
37	H+C2H2=C2H3	12.74	0.00	2.5	12.95	0.02	43.7	29
38	C2H3+H=H2+C2H2	13.00	0.00	0.0	12.87	0.13	62.8	29
39	H2=2H	12.35	-.50	92.5	12.27	-0.65	-11.5	29
40	C2H2=C2H+H	16.62	0.00	107.0	11.79	0.96	-20.6	29
41	2C2H2=NC4H3+H	12.30	0.00	45.9	14.18	-0.70	-23.1	29
42	I-C4H3+H2=C2H2+C2H3	10.70	0.00	20.0	10.08	0.37	16.1	9
43	C4H4=I-C4H3+H	15.20	0.00	85.0	9.69	0.84	-14.4	9
44	C4H4=NC4H3+H	15.00	0.00	100.0	10.62	0.65	-9.5	9
45	C2H+C4H4=C2H2+I-C4H3	13.60	0.00	0.0	12.91	-0.12	28.2	29
46	NC4H3=C2H2+C2H	14.30	0.00	57.0	7.59	1.66	-1.6	9
47	I-C4H3=C4H2+H	12.00	0.00	49.0	11.99	0.24	-0.9	9
48	NC4H3=C4H2+H	12.60	0.00	40.0	11.46	0.44	0.2	9
49	NC4H3+H=I-C4H3+H	13.48	0.00	0.0	12.34	0.20	10.1	9
50	I-C4H3+H=C4H2+H2	13.00	0.00	0.0	13.08	0.39	54.1	9
51	NC4H3+H=C4H2+H2	13.00	0.00	0.0	11.94	0.59	64.2	9
52	C4H4+H=I-C4H3+H2	14.49	0.00	14.5	9.06	0.99	19.1	9
53	C4H4+H=NC4H3+H2	13.90	0.00	14.5	9.60	0.79	9.0	9
54	C2H3+C2H2=NC4H5	12.04	0.00	4.0	21.03	-2.02	43.4	9
55	C2H+H2=H+C2H2	12.85	0.00	0.0	17.59	-1.11	23.6	28
56	C2H+C2H2=C4H2+H	13.60	0.00	0.0	19.17	-1.22	18.8	29
57	C4H2=C4H+H	14.89	0.00	120.0	10.29	0.83	-0.2	28
58	C2H+C4H2=C6H2+H	13.60	0.00	0.0	19.77	-1.34	18.8	29
59	C4H+C2H2=C6H2+H	13.30	0.00	0.0	19.25	-1.21	11.4	9
60	C6H2=C6H+H	14.89	0.00	120.0	10.81	0.62	3.6	28
61	C4H+H2=H+C4H2	13.30	0.00	0.0	17.82	-0.98	16.2	28
62	C6H+H2=H+C6H2	13.30	0.00	0.0	17.30	-0.77	12.4	28
63	C2H+H=C2+H2	12.00	0.00	23.0	8.71	0.79	1.6	9
64	C2H+M=C2+H+M	16.67	0.00	124.0	13.30	0.65	-1.4	30

* NOTES: Units for A: cc,moles,sec.
Units for E: kcal/mole.
"=" indicates forward and reverse rates included in the model
"-" indicates forward rate only included in model
PW indicates rate evaluated from the present work
BA = biacetyl (CH3COCOCH3)
AT = acetone (CH3COCH3)
Reverse rates calculated from forward rates and thermchemistry

TABLE I (continued)
SET OF REACTIONS AND RATE COEFFICIENTS
logk = logA + nlogT - E/(2.303RT) *

	Reactions	Forward rate constant			Reverse rate constant			
		A	n	E	A	n	E	Ref
65	C2H+C6H6=C6H5+C2H2	13.30	0.00	0.0	12.00	0.01	14.0	31
66	C4H+C6H6=C6H5+C4H2	13.30	0.00	0.0	11.77	0.14	6.6	31
67	C2H3+C4H2=C4H4+C2H	13.48	0.00	23.0	13.96	-0.14	3.5	9
68	C6H6=C6H5+H	16.18	0.00	107.9	10.04	0.98	-5.7	32
69	C6H6+H=C6H5+H2	14.40	0.00	16.0	8.35	1.12	6.4	31
70	2C6H5=C12H10	12.48	0.00	0.0	27.96	-3.17	117.1	4
71	C6H5+C6H6=C12H10+H	11.80	0.00	11.0	21.15	-2.20	14.5	33
72	NC4H3+C6H5=C10H8	13.00	0.00	0.0	33.05	-3.44	173.9	9
73	C2H2+C6H5=C8H6+H	12.00	0.00	4.0	20.27	-1.89	8.4	34,9
74	C2H4+C6H5=C8H8+H	11.57	0.00	2.1	20.88	-2.20	7.7	34
75	C2H3+C4H4-C6H6+H	11.60	0.00	0.0	0.00	0.00	0.0	9
76	NC4H5=C4H4+H	14.00	0.00	41.4	11.06	0.66	1.4	35
77	NC4H5+C2H2-C6H6+H	12.81	0.00	9.0	0.00	0.00	0.0	9
78	NC4H5+H=C4H4+H2	13.00	0.00	0.0	10.15	0.80	64.0	9
79	C4H6+H=NC4H5+H2	14.00	0.00	14.5	9.52	0.91	8.6	9
80	C6H6+C2H=C8H6+H	12.00	0.00	0.0	18.97	-1.87	18.4	9
81	C4H4=C2H+C2H3	16.00	0.00	105.0	5.12	2.33	-21.9	9
82	C4H4+NC4H5-C8H8+H	13.90	0.00	3.0	0.00	0.00	0.0	9
83	C8H8+H-C8H6+H+H2	14.60	0.00	7.0	0.00	0.00	0.0	9
84	C6H5+C2H3=C8H8	13.00	0.00	0.0	27.36	-3.07	112.9	9
85	L-C6H5=NC4H3+C2H2	14.00	0.00	36.0	4.63	1.97	-5.6	9
86	C6H5=L-C6H5	13.54	0.00	65.0	12.66	-0.68	3.3	9

* NOTES: Units for A: cc,moles,sec.
Units for E: kcal/mole.
"=" indicates forward and reverse rates included in the model
"-" indicates forward rate only included in model
PW indicates rate evaluated from the present work
BA = biacetyl (CH3COCOCH3)
AT = acetone (CH3COCH3)
Reverse rates calculated from forward rates and thermchemistry

List of Figures

FIG. 1

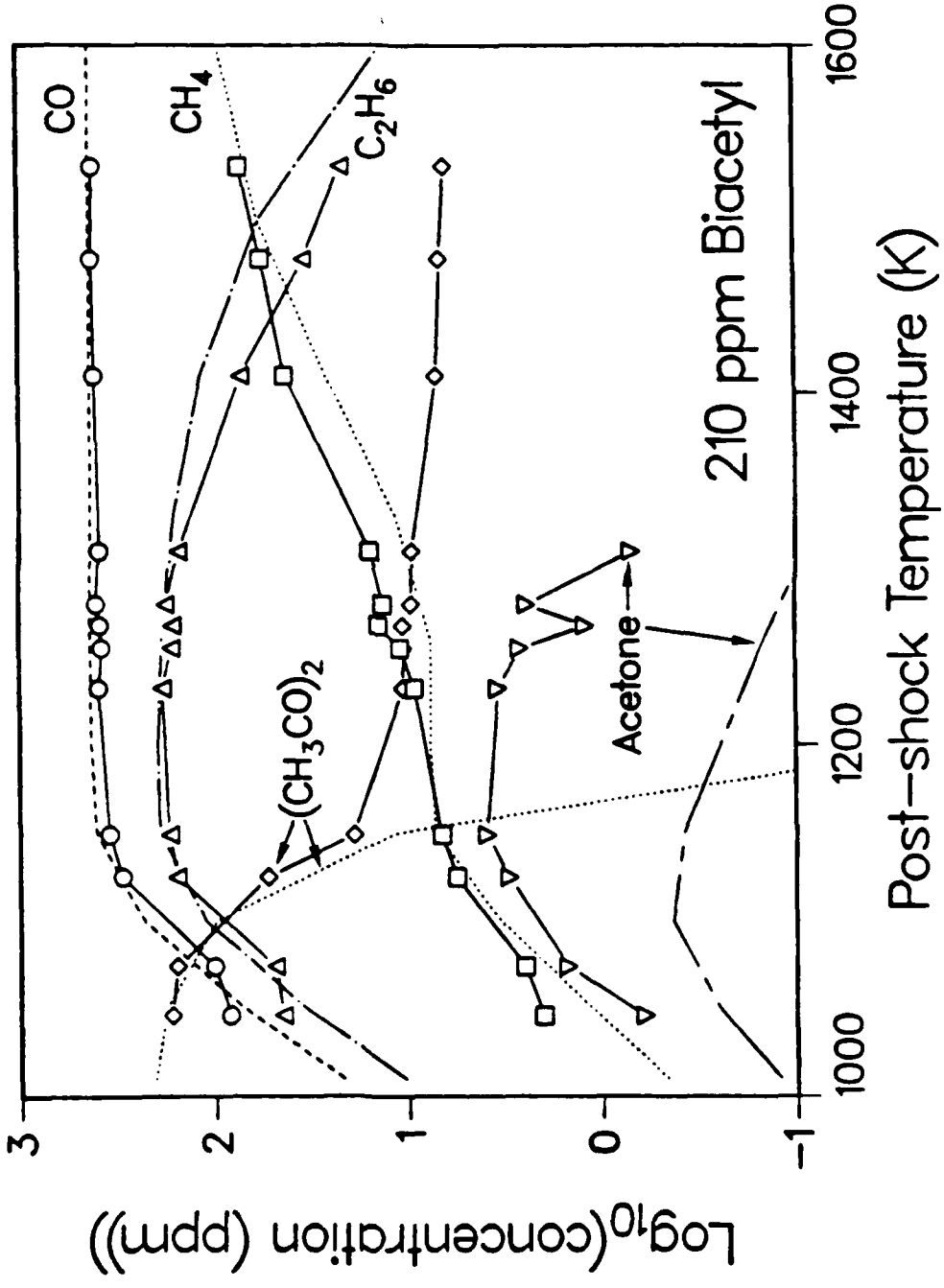
CO
CH4
C2H6
(CH3CO)2
Acetone
210 ppm Biacetyl
Log10(concentration (ppm))
Post-shock Temperature (K)
3
2
1
0
-1
1000
1200
1400
1600

FIG. 2

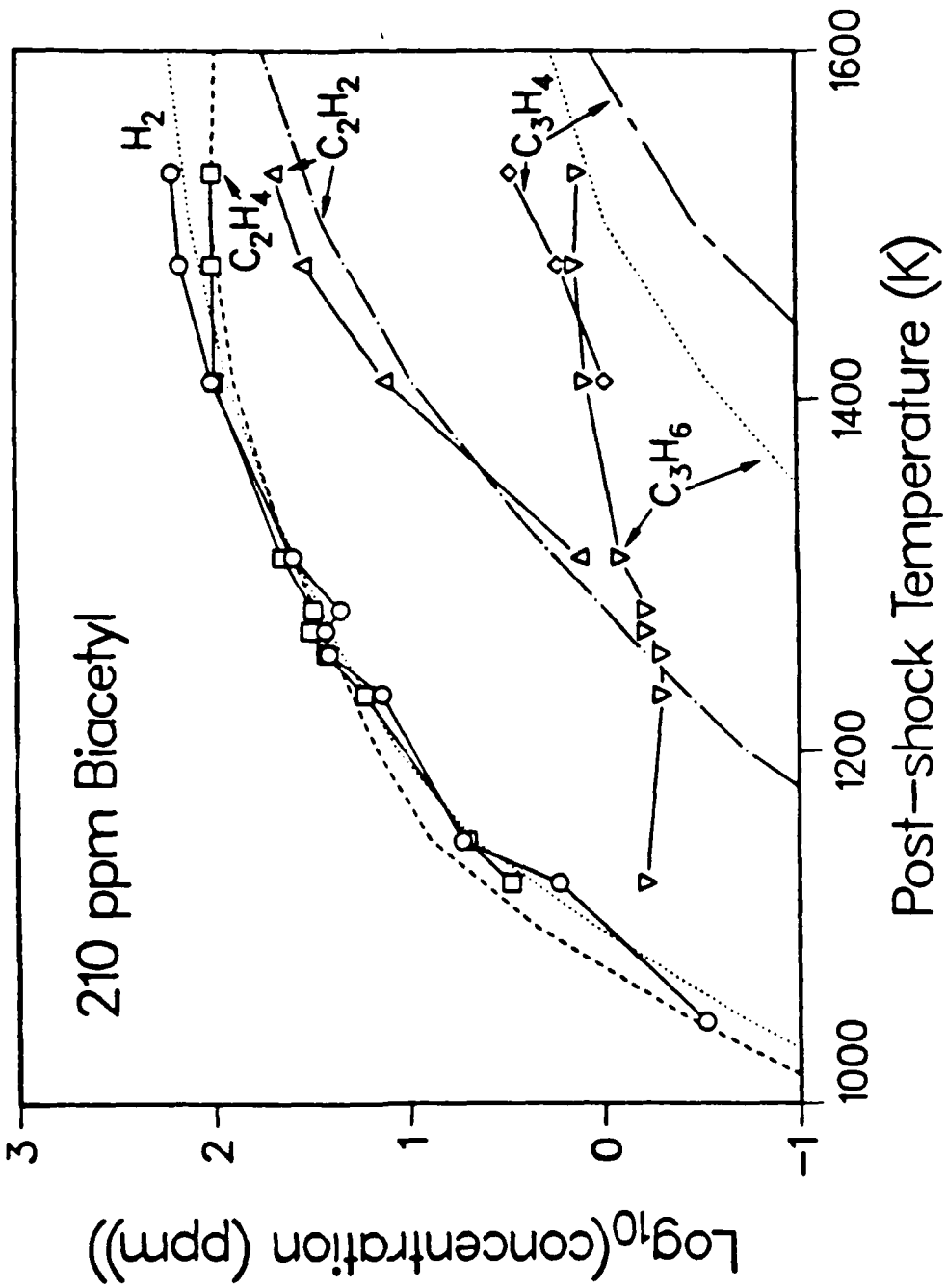
210 ppm Biacetyl
H_2
C_2H_4
C_2H_2
C_3H_4
C_3H_6
Log_{10}(concentration (ppm))
3
2
1
0
−1
1000
1200
1400
1600
Post−shock Temperature (K)

FIG. 3

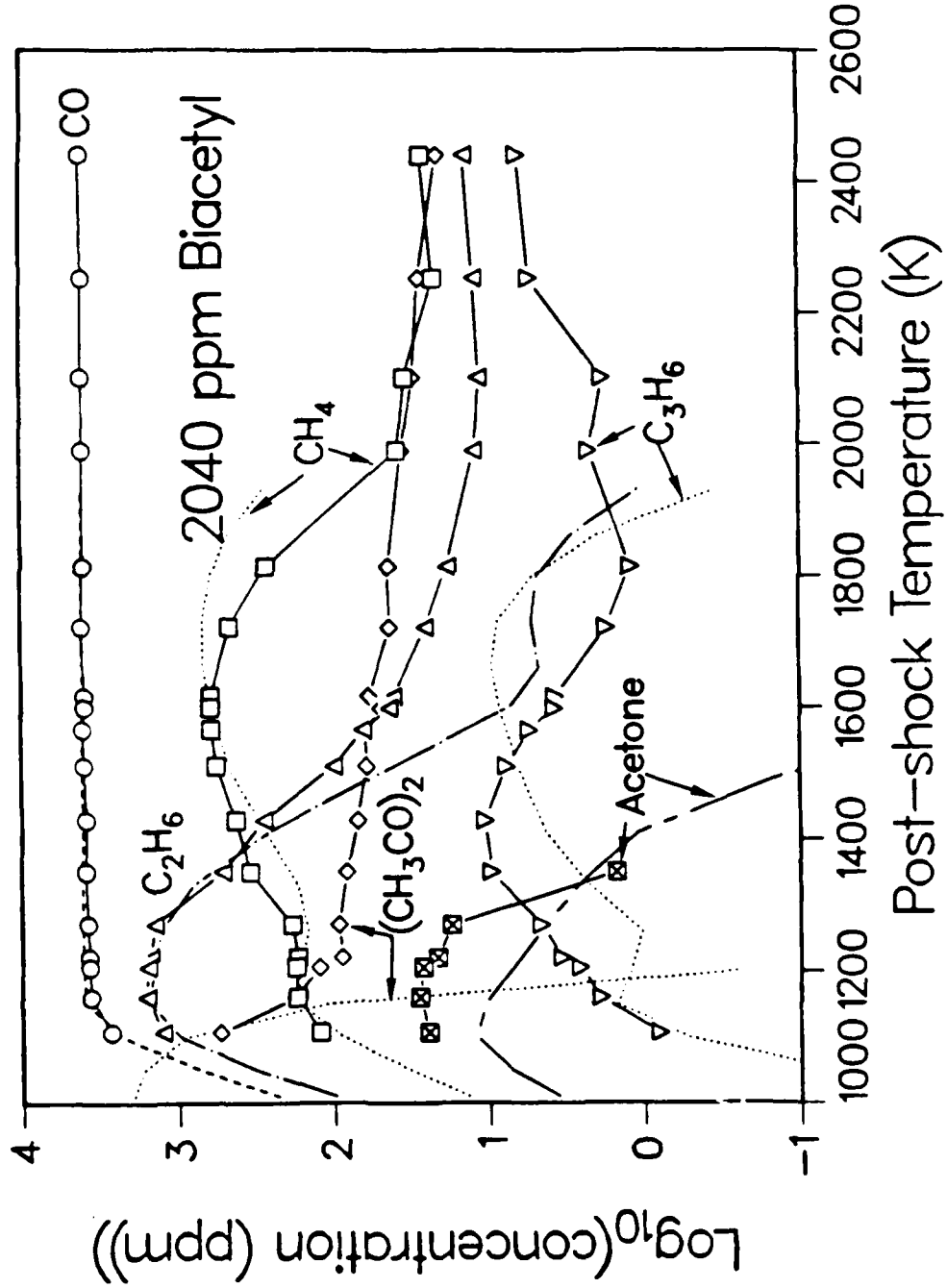
2040 ppm Biacetyl
CO
C_2H_6
CH_4
$(CH_3CO)_2$
Acetone
C_3H_6
Log_{10}(concentration (ppm))
Post-shock Temperature (K)
4
3
2
1
0
−1
1000
1200
1400
1600
1800
2000
2200
2400
2600

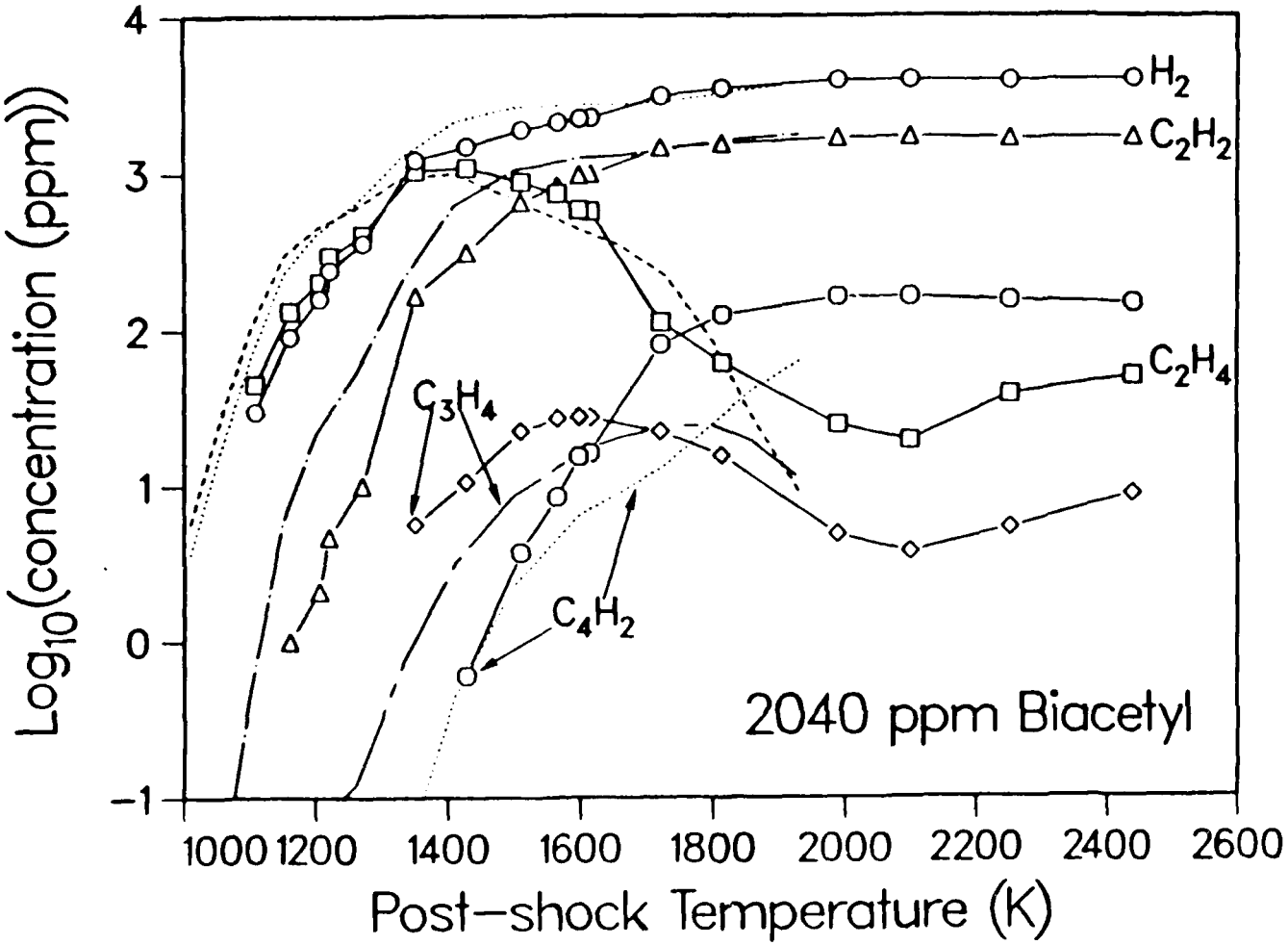
4
3
2
1
0
−1
Log10(concentration (ppm))
1000 1200 1400 1600 1800 2000 2200 2400 2600
Post−shock Temperature (K)
H2
C2H2
C2H4
C3H4
C4H2
2040 ppm Biacetyl

FIG. 5

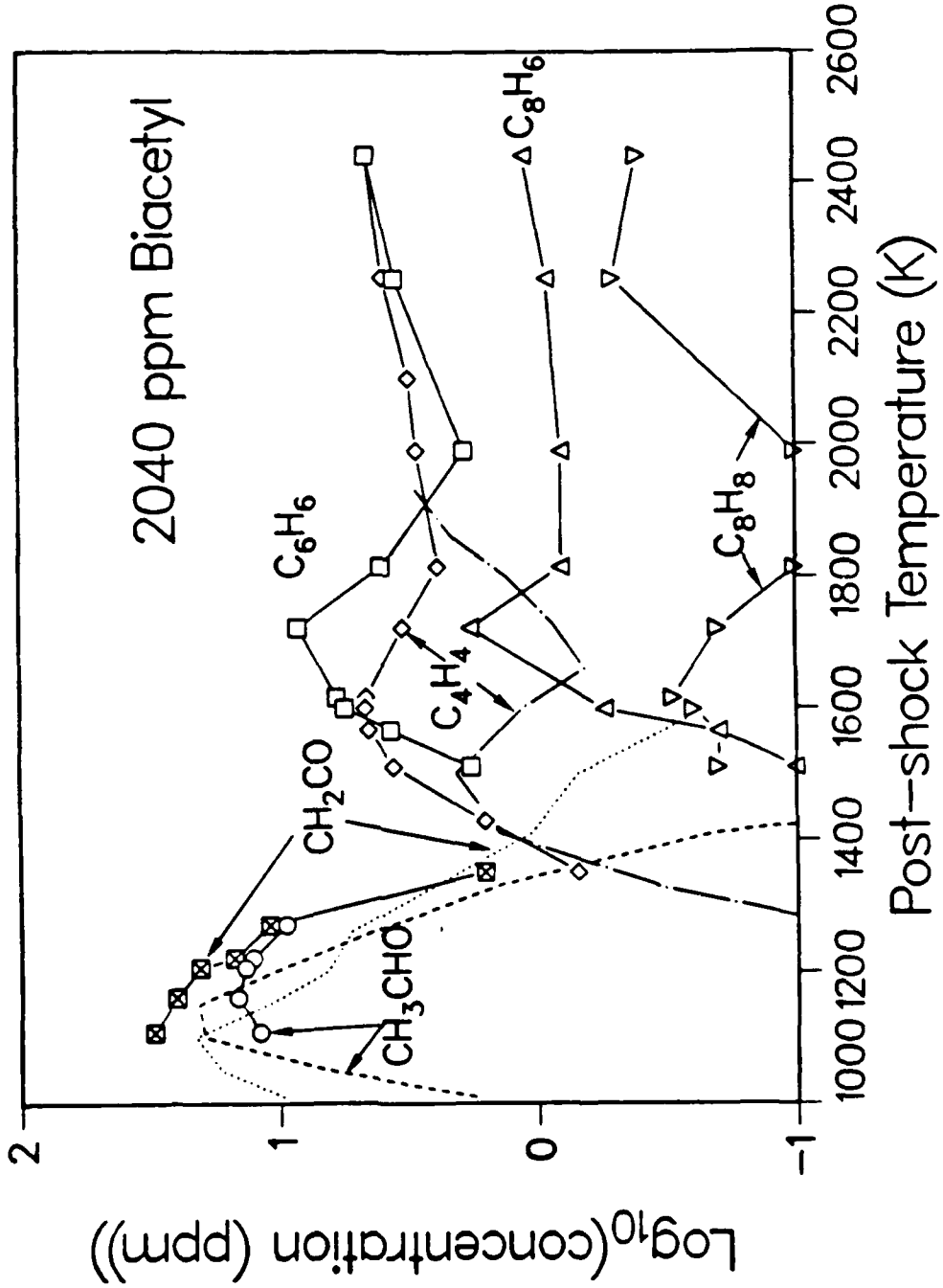
2040 ppm Biacetyl
C_6H_6
C_8H_6
C_4H_4
CH_2CO
C_8H_8
CH_3CHO
Log10(concentration (ppm))
2
1
0
−1
1000 1200 1400 1600 1800 2000 2200 2400 2600
Post−shock Temperature (K)

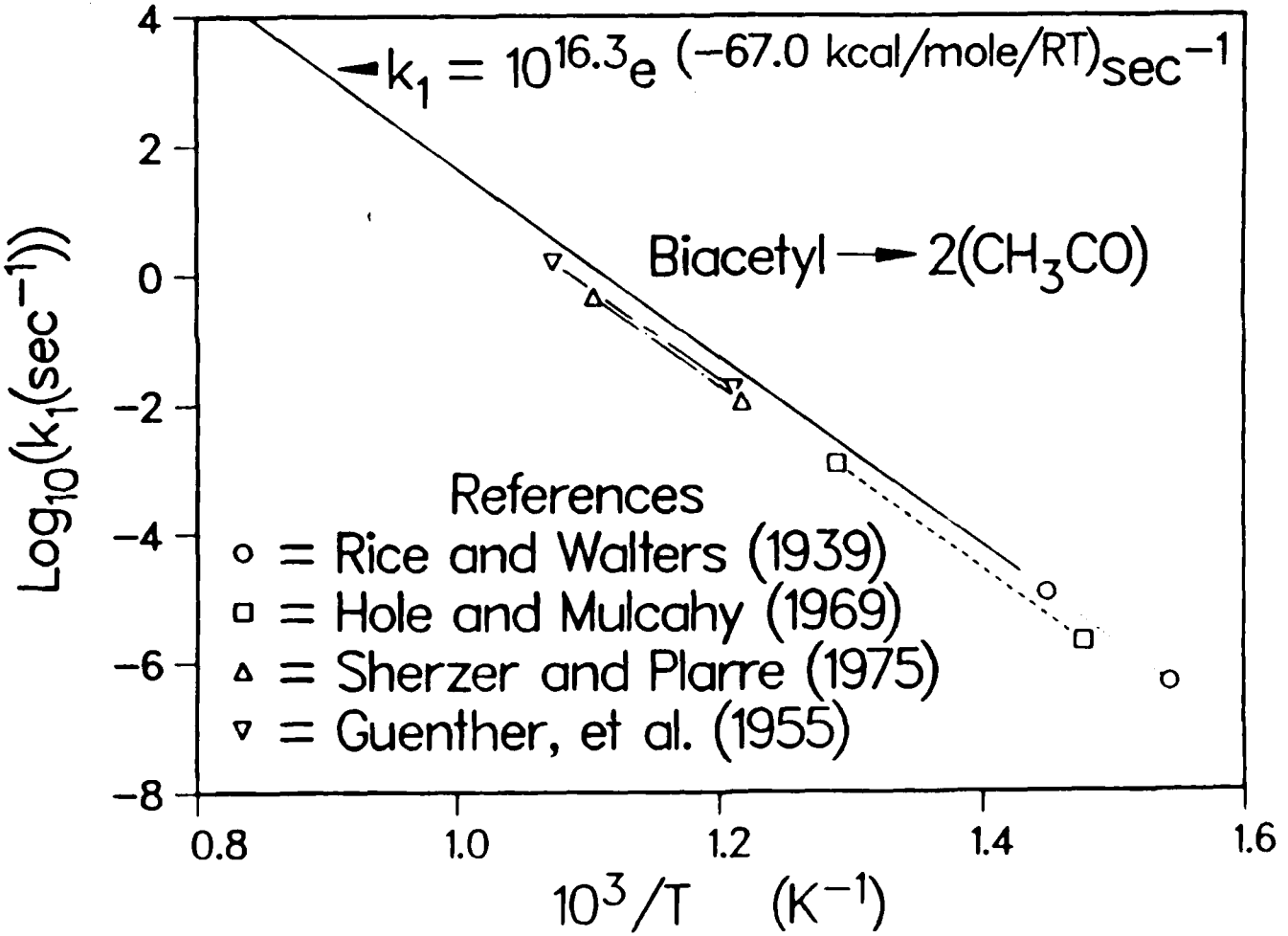
$k_1 = 10^{16.3} e^{(-67.0 \text{ kcal/mole/RT})} \text{sec}^{-1}$
Biacetyl → 2(CH_3CO)
References
○ = Rice and Walters (1939)
□ = Hole and Mulcahy (1969)
△ = Sherzer and Plarre (1975)
▽ = Guenther, et al. (1955)
$\text{Log}_{10}(k_1(\text{sec}^{-1}))$
4
2
0
−2
−4
−6
−8
0.8
1.0
1.2
1.4
1.6
$10^3/T$ (K^{-1})

FIG. 6

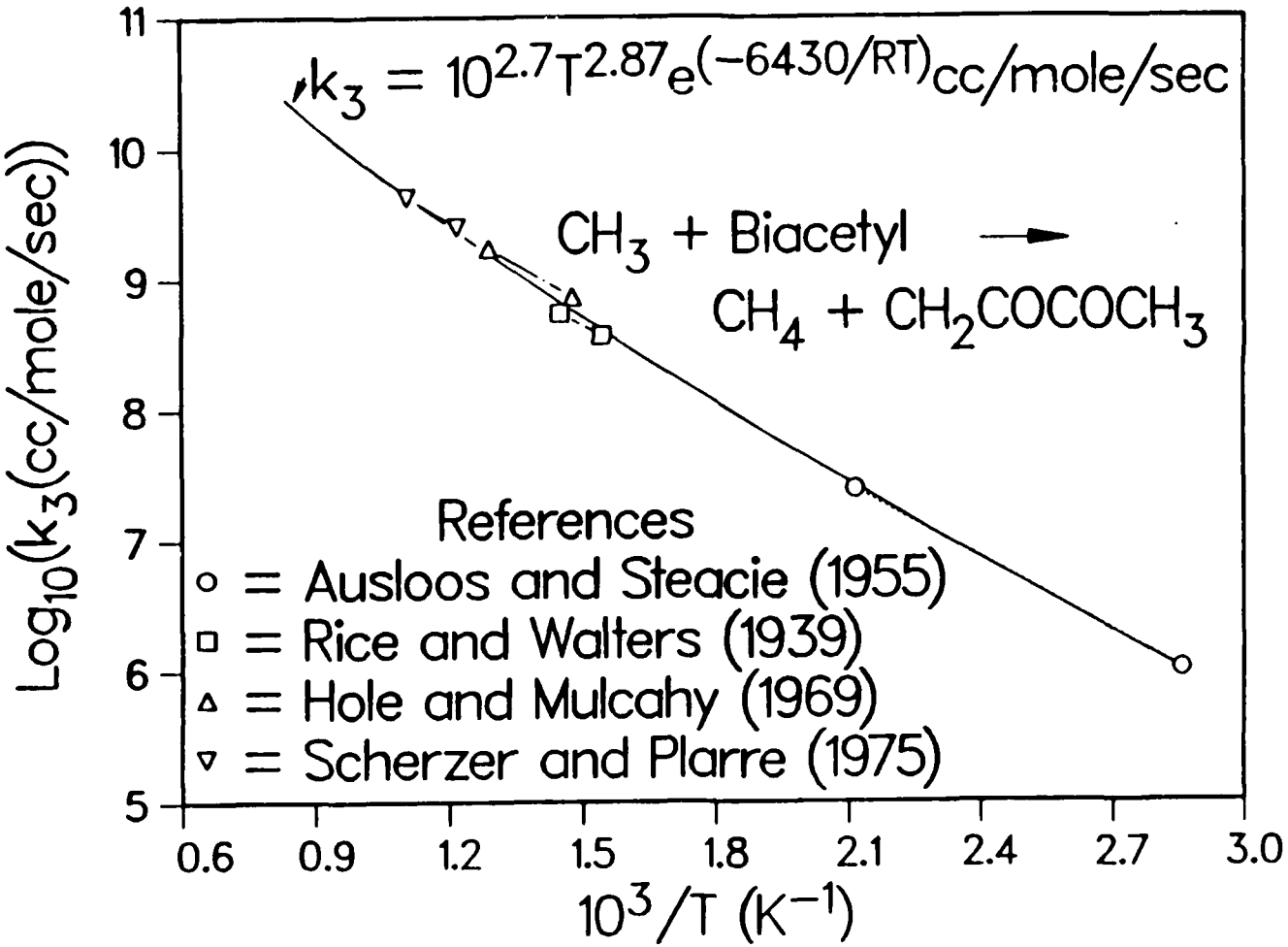
$k_3 = 10^{2.7}T^{2.87}e^{(-6430/RT)}$cc/mole/sec
CH_3 + Biacetyl →
CH_4 + $CH_2COCOCH_3$
References
○ = Ausloos and Steacie (1955)
□ = Rice and Walters (1939)
△ = Hole and Mulcahy (1969)
▽ = Scherzer and Plarre (1975)
$Log_{10}(k_3(cc/mole/sec))$
11
10
9
8
7
6
5
0.6
0.9
1.2
1.5
1.8
2.1
2.4
2.7
3.0
$10^3/T\ (K^{-1})$

FIG. 7

FIG. 8

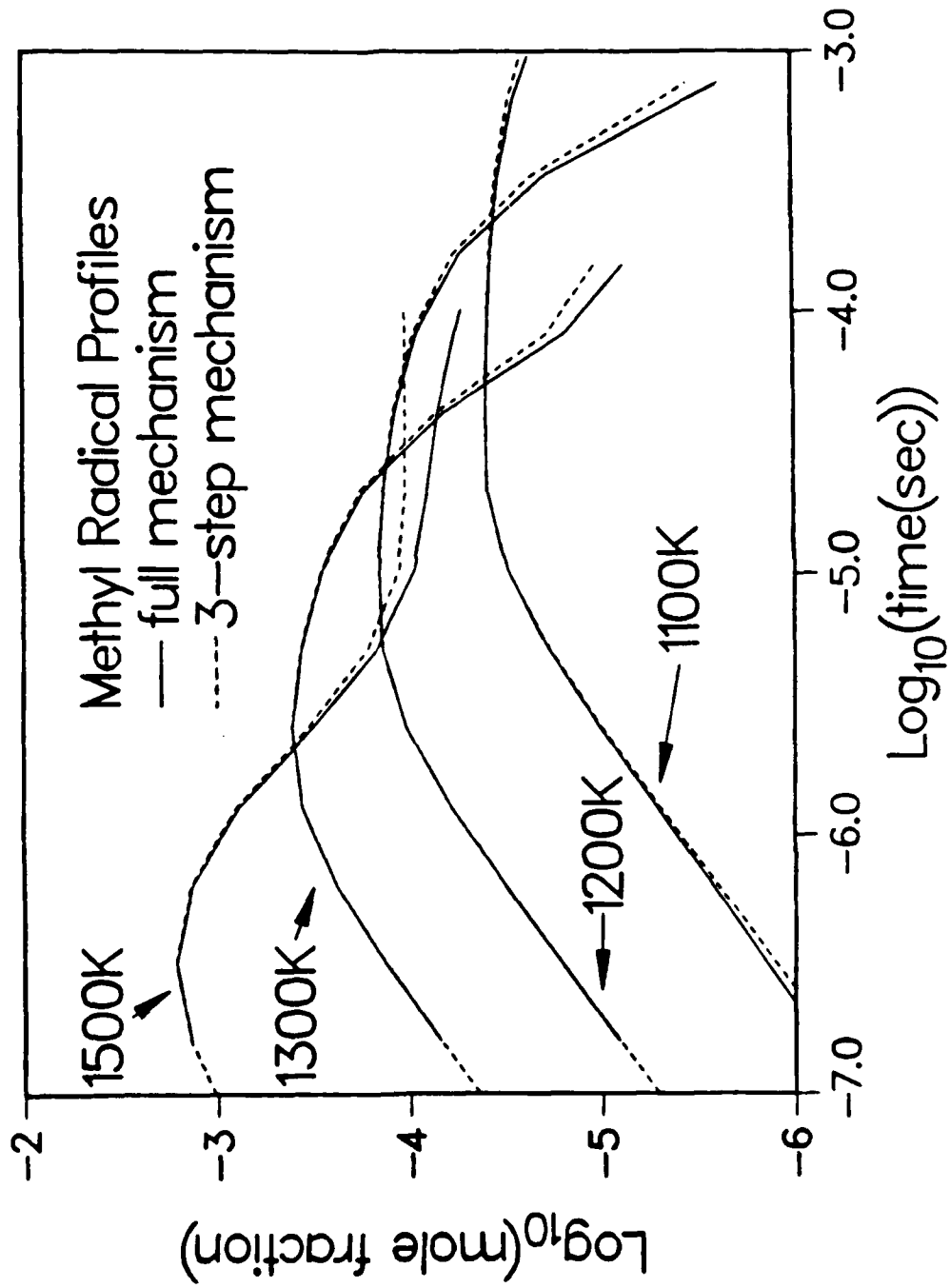
Methyl Radical Profiles
— full mechanism
---- 3-step mechanism
1500K
1300K
1200K
1100K
Log10(mole fraction)
Log10(time(sec))
-2
-3
-4
-5
-6
-3.0
-4.0
-5.0
-6.0
-7.0

END

4-87

DTIC